

“Macrophage-induced myofibroblasts migration via paracrine signaling using 3D scaffolds with variable fiber alignment and cyclic stretch”

Master Thesis
Sparla, J.K.W.

Prof. Dr. C.V.C. Bouten
Dr. Ir. A.I.P.M. Smits
Dr. Ir. N.A. Kurniawan
Dr. Ir. D. Gawlitta
Ir. E.E. van. Haften

1 Abstract

The biggest problem of arteriovenous-grafts (AVGs), used to create blood flow access for end stage renal disease (ESRD) patients, is the occurrence of neo-intimal hyperplasia leading to venous stenosis. This process is caused by the migration of smooth muscle cells (SMCs) and myofibroblasts from the media into the intima layer and is thought to be caused by vascular injury (e.g. as a result of implantation) or damage to the endothelial layer.

Novel approaches to gain vascular access and additionally avoid neo-intimal hyperplasia, involve the use of in-situ tissue engineering (TE). In-situ TE relies on the implantation of resorbable biomaterials causing endogenous tissue regeneration, gradually transforming into an homeostatic replacement tissue.

The implantation of any material in the human body causes a foreign body response (FBR) in which macrophages are key players. These macrophages have the ability to direct migration for myofibroblasts and SMCs, highlighting their involvement in neo-intimal hyperplasia. Macrophages are a plastic cell type, for which the phenotype is generally described by the canonical pro-inflammatory (M1) or anti-inflammatory (M2) paradigm. Physiologically this phenotype is determined by chemical stimulation via soluble factors secreted by other cells, but macrophage polarization can be altered by physical factors such as cyclic strain or microarchitecture of an implanted synthetic AVG.

In this study, the effects of macrophage polarization under the influence of biochemical or physical factors (i.e. cyclic strain and scaffold microarchitecture) on the migration of myofibroblasts were investigated. These HVSCs were stimulated to migrate through 8 μ m pore sized Transwell membranes by using macrophage-conditioned media (MCM). MCM was obtained through either biochemical stimulated peripheral blood mononuclear cells (PBMCs) culture via IL-4 (M2) or IFN- γ (M1) or through physically stimulated PBMCs, by seeding them on scaffolds with different degrees of anisotropy and applying cyclic strain.

Results showed no significant effects of the different fiber orientations in both statically and strained culture groups. Applying cyclic strain a 7% seemed to play a bigger role, causing an increase in HVSC migration compared to statically cultured groups. Immunology results for cyclically strained groups showed an overall decrease in CD163 (M2 marker) expression. On top of this, qPCR results for isotopically aligned scaffold strips exposed to strain showed an overall decrease in both M1 and M2 markers, suggesting an upregulated HVSC migration response due to a decrease in M2 polarized macrophages. Moreover, biochemically induced M1-polarized MCM seemed to demonstrate an increased HVSC migration response compared to positive control (significant), M0 MCM (unstimulated macrophages, non-significant) and M2 MCM (non-significant).

Overall results propose M1 macrophages to play a bigger role in causing neo-intimal hyperplasia compared to other phenotypes, yet further experiments are needed to confirm these observed effects.

Contents

1	Abstract.....	2
2	Introduction	4
3	Materials and Methods.....	6
3.1	Experimental outline.....	6
3.2	Cell culture and seeding.....	7
3.2.1	Macrophages.....	7
3.2.2	Human vena saphena cells.....	8
3.3	Analyses	9
3.3.1	Migration.....	9
3.3.2	Gene expression.....	9
3.3.3	Immunofluorescence	11
3.4	Statistics	11
4	Results.....	12
4.1	Scaffold characterization and strain validation	12
4.1.1	Scaffold sheet characterization.....	12
4.1.2	Scaffold strain validation.....	13
4.1.3	Transwell chemotactic gradient validation.....	14
4.2	Biochemically stimulated macrophages	15
4.2.1	Phenotypical characterization- qPCR.....	15
4.2.2	HVSC migration- biochemically stimulated MCM.....	16
4.3	Physically stimulated macrophages.....	17
4.3.1	Phenotypical characterization- qPCR.....	17
4.3.2	Phenotypical characterization- Immunofluorescence	17
4.3.3	HVSC migration- Physically stimulated MCM	19
5	Discussion.....	20
6	Conclusion.....	23
7	References	24
8	Appendices.....	27

2 Introduction

Approximately 1% of the population suffers from renal failure, with 2000 new patients every year in the Netherlands alone.¹ Chronic kidney disease (CKD) is a state in which progressive loss of kidney function occurs. If left untreated, this may result in death. In the final stage of this disease, defined as end stage renal disease (ESRD), patients rely on renal replacement therapies or haemodialysis.^{2,3} Via a minor surgery in the forearm of a patient, haemodialysis access is created and circulatory blood is filtered via a dialysis machine.⁴ Currently, the golden standard to create haemodialysis access is either directly connecting an artery to a vein creating an arteriovenous fistula (AVF). AVFs cannot be used acutely but require a maturation phase of three to four months to adjust to the augmented blood flow and to induce vessel wall thickening.⁵

Alternatively to an AVF, vascular access can be created by connecting an artery and a vein via a synthetic tubular construct called an arteriovenous-graft (AVG).^{5,6} AVGs, however, face a high incidence of thrombosis, infection and the occurrence of neo-intimal hyperplasia leading to venous stenosis.⁷

Neo-intimal hyperplasia is caused by the migration of smooth muscle cells (SMCs) and myofibroblasts from the media into the intima layer.⁸ The exact underlying cause for the migration of these two cell types remains unknown. However, it is hypothesized that vascular injury (e.g. as a result of implantation) or damage to the endothelial layer leading to altered fluid flow and shear stress can be sensed by SMCs and myofibroblasts, causing these cells to migrate.⁸

Novel approaches to gain vascular access involve the use of in-situ tissue engineering (TE). In-situ TE relies on the implantation of resorbable biomaterials causing endogenous tissue regeneration, gradually transforming into an homeostatic replacement tissue.⁹ Since these biomaterials, called scaffolds, can also be created in advance and implanted on demand, in-situ TE AVGs have the option of acute usage, with the added benefit of transforming into endogenous tissue.

The implantation of any foreign materials, including scaffolds for in-situ tissue engineered AVGs, are bound to evoke a host inflammatory response also known as the foreign body response (FBR).¹⁰ This is a series of cell-based signaling events in which macrophages are key players by mediating the degradation of the scaffold material, as well as the formation and remodeling of tissue via the secretion of growth factors or cytokines.

Macrophages have a functional plasticity dependent on physical and chemical properties of the environment. These cells are generally classified in two phenotypes; a pro inflammatory phenotype (M1 macrophage) and a pro-wound healing phenotype (M2 macrophage). M2 macrophages can be sub-divided into at least three functionally different phenotypes (M2a, M2b and M2c). However, all these different macrophage phenotypes tend to overlap, making it difficult to identify individual macrophage phenotype.¹¹ Nevertheless, the balance between M2/M1 macrophages present in implanted biomaterials during the FBR is a predictor for long term tissue outcome.⁹ Therefore, modulating this balance towards pro-wound healing, is a key target to guide functional tissue regeneration.⁹

Cytokines like interleukin-4 (IL-4) can stimulate macrophages to assume an M2-phenotype, whilst Interferon- γ (IFN- γ) has been shown to induce M1-polarization.¹² Additionally, physical stimuli including shear and strain can also influence macrophage polarization. Application of cyclic stretch to macrophages in physiological ranges (5-12%), has been shown to directly affect macrophage phenotype^{13,14}. Strains of 7% guided macrophage polarization to the M2 phenotype, whilst strains of 12% decreased M2 phenotype occurrence.¹³

Macrophages being the key players of the FBR, interact with many different cell types, including SMCs and myofibroblasts and are able to direct migration for these cell types²¹ (depicted in figure 1). This makes modulation of macrophage phenotype an interesting target to prevent neo-intimal hyperplasia.

The aim of this study was to investigate the effect of macrophage phenotype affecting factors (chemical stimuli, fiber alignment and cyclic stretch) on the migration of myofibroblasts. This can, in turn, provide more insight in neointimal hyperplasia and its underlying causes.

Based on previous research obtained through co-culture experiments, it is expected that macrophages with anti-inflammatory characteristics (M2) induce the most myofibroblasts, SMCs migration compared to unstimulated (M0) or M1 stimulated macrophages.²² Building on this, it is expected that macrophages cultured on scaffolds with anisotropically aligned fibers exposed to cyclic strains of 7% causes an increase in M2 macrophage polarization and consequently cause an increase in myofibroblasts migration.

To test this hypothesis, human vena saphena cells (HVSCs) will be stimulated to migration by macrophage-conditioned media (MCM) in a modified Boyden chamber experiment.²³ These HVSCs are cells derived from the saphenous vein and are comparable to myofibroblasts.²⁴ MCM will be created by culturing macrophage and either biochemically stimulating them with IL-4 (M2) or IFN- γ (M1) or physically stimulating them in cyclically stretched (~7%) fibrous polycaprolactone bis-urea (PCL-BU) scaffolds with different fiber orientations.

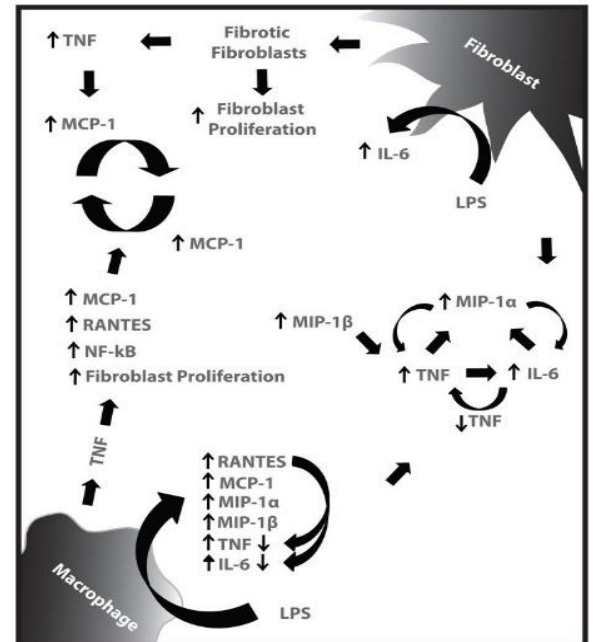


Figure 1, different signaling interactions between macrophages and fibroblasts^{15,19}

3 Materials and Methods

3.1 Experimental outline

HVSCs were seeded on top of 8µm pore sized Transwells and stimulated to migration by macrophage-conditioned media (MCM) in a modified Boyden chamber experiment (Figure 2)²³. To obtain this MCM, primary human macrophages were either biochemically stimulated with IL-4 (M2) or IFN-γ (M1) or physically stimulated in cyclically stretched (~7%) fibrous scaffolds. The phenotype of cultured macrophages was checked with immunofluorescence and qPCR. The scaffolds were prepared from polycaprolactone bis-urea (PCL-BU) with different fiber orientations to also assess the effect of microarchitecture.²⁵

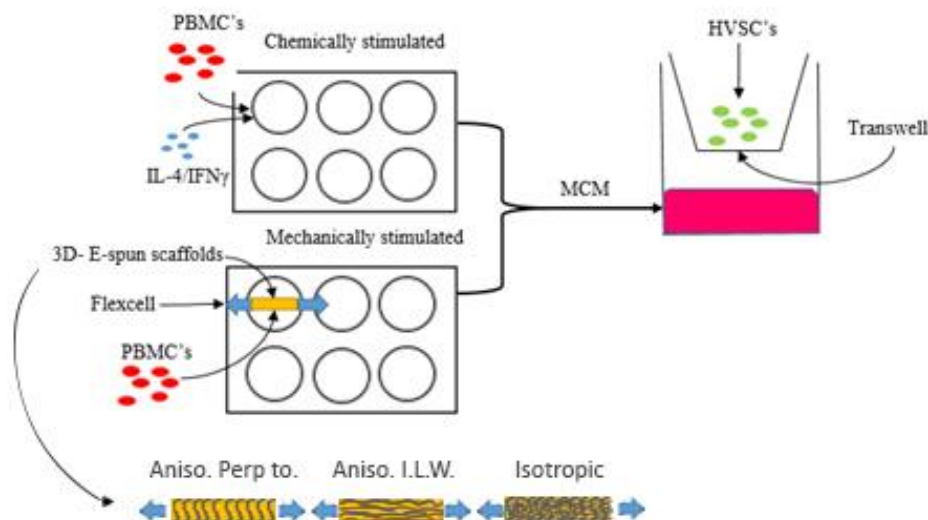


Figure 2, Scheme displaying experimental plan, PBMCs are cultured and stimulated biochemically (with IL-4 or IFN-γ) or physically. Physical stimulation is achieved by seeding PBMCs on 3D-electrospun scaffolds with different fiber orientations (Anisotropic perpendicular to strain, anisotropic in line with strain and isotropic) and exerting cyclic strain onto these scaffolds. Macrophage-conditioned media from both cultures is used to stimulate HVSC migration through a Transwell membrane.

Scaffolds were produced using electrospinning from a thermoplastic elastomer based on poly-ε-caprolactone PCL2000 soft block and a 1,4-bis-ureido butane hard block (PCL-BU). The polymer was dissolved at 15 % (w/w) in a solution containing amylene stabilized chloroform (CHCl₃; Sigma, 372978) and methanol (MeOH; Sigma, 322415-2L). For the creation of anisotropic aligned sheets, a combination of 99% CHCl₃ and 1% MeOH was used, whereas for isotropic aligned sheets 2% MeOH was used.

The polymer solution was introduced into the electrospinning device (EC-CLI, IME, Technologies, Geldrop, The Netherlands) system via a syringe and pump system. Via this pump system, the solution was pulled through a positively charged nozzle and collected on a negatively charged rotating mandrel. Different polymer solutions were then used to create the differently aligned sheets using the electrospinning device. Besides polymer solution ratios, device settings like the rotation speed of the mandrel and the voltage applied to the nozzle and mandrel were varied in order to produce the different scaffold sheets (table 1).

Scaffold	Voltage (kV)	Working distance (cm)	Flow rate (µl/min)	Gas shield (ml/min)	Temperature(°C)/ Humidity (%)	Target diameter (mm)	Mandrel RPM
Anisotropic	17	16	40	30	23/ 30	35	2300
Isotropic	20	16	40	30	23/ 30	35	100

Table 1, Electrospinning parameters used as input to spin anisotropic or isotropic scaffold sheets

After spinning, scaffolds were dried overnight in vacuum at room temperature to avoid polymer shrinkage during experiments. Scaffold strips of 25x5x0.3 mm were cut out of the electrospun sheets, glued at the ends to non-coated Bioflex 6 well culture plates (Dunn labortechnik, BF-3001U) using Silastic MDX4-4210 (Dow Corning, Michigan, USA) and cured at 65 °C for 90 min.

Scaffold thickness was determined by using the build-in laser on the Electrospinning device and further confirmed via digital microscopy using build-in measuring software on the Keyence microscope (VHX-500FE, Keyence, Mechelen, Belgium). Fiber diameter and degree of anisotropy were quantified from scanning electron microscopy images (SEM, Quanta 600F, GEI, Eindhoven). Fiber diameter was determined by averaging 10 different fibers in images, whereas the degree of anisotropy was determined by using a Matlab code previously described in van Haaften et al., 2018.²⁶

3.2 Cell culture and seeding

3.2.1 Macrophages

3.2.1.1 Biochemical stimulation

PBMCs were seeded on polystyrene 6 well culture plates (Greiner, 657185) with a density of 1.5×10^6 PBMCs/cm², seeding a total of 14.25×10^6 PBMCs/well. PBMCs were cultured in macrophage colony-stimulating factor (M-CSF; Invitrogen, PHC9504) enriched RPMI media (Gibco, 12633-012) containing 20% fetal bovine serum (FBS; Greiner Bio-one, 26140079), 1% penicillin/streptomycin (P/S; Lonza, 17-602E) and 100ng/ml M-CSF for 7 days to induce monocyte-to-macrophage differentiation. It was assumed that only monocytes are able to adhere to the bottom of the wells plates, removing all non-monocytes from the PBMC population after the first wash (at day 1). Media was refreshed at day 4 and 7. At day 7, cells were polarized for 18 hours in media containing RPMI + 5% FBS + 1% P/S + either 20ng/ml IFN- γ (M1), 20ng/ml IL-4 (M2) or neither (M0). After 18 hours of stimulation, the conditioned medium was collected, centrifuged at 350g for 7 minutes to remove cellular remnants and the supernatant was stored at -80°C until use. After media aspiration, wells were washed twice with sterile phosphate buffered saline (PBS; Sigma, P-4417) and 600 μ l of RLT buffer was added. Wells were plated on ice and cells were scraped from the bottom of each wells plate. The lysed cells in RLT were stored at -20°C for gene expression analysis (section 4.2)

3.2.1.2 Physical stimulation

The scaffold strips glued onto Bioflex plates were sterilized by UV irradiation (2x 5minutes) followed by 30 minutes of 70% ethanol incubation. After sterilization, the scaffolds were washed twice with sterile PBS and incubated overnight with RPMI media containing 10% FBS and 1% P/S (Macrophage culture medium), to allow for protein adsorption. PBMCs were seeded in the scaffolds using fibrin as a cell carrier. In short, cells were mixed at a concentration of 5×10^5 cells/ μ l in thrombin (Sigma, T-4648; 10U/ml), mixed with fibrinogen (Sigma, F3879; 10mg/ml), and carefully pipetted onto the pre-wetted scaffolds strips up to a total seeding density of a $\sim 15 \times 10^6$ cells/strip. The fibrin was allowed to polymerize for 15 minutes in a standard incubator (37 °C, 5% CO₂). After polymerization, 3ml macrophage culture media was added to each well and scaffolds were cyclically loaded at 7% strain using the Flexcell FX-5000 Tension system (Flexcell International Corporation, NC, USA). Media was replaced at day 1 with fresh media to remove the non-adherent PBMC cell fraction. At day 3 of straining, scaffolds were cut out of the Bio flex plates and were either snap-frozen in liquid N₂ and stored at -80 °C (qPCR) or fixed for 10 minutes using 3.7% Formaldehyde solution, washed in PBS, and stored at 4 °C (Staining).

In order to determine the Flexcell software strain settings corresponding to 7% scaffold strain, control experiments were performed on bare scaffolds.

In short, contrast was applied to bare scaffold strips (using graphite) after which short movies of 3-5 strain cycles were made at different software strain levels, ranging from 3 to 7%.

Using Matlab code software (Appendix A.1.1), the Green-Lagrange strain exerted onto those scaffold strips was calculated at every frame in one cycle by tracking the displacements of set points.²⁷ During cell culture experiments, a graphite stained control sample was included in each experiment and strain was checked daily.

3.2.2 Human vena saphena cells

Human vena saphena cells (HVSCs) of passage 4 and 5 were cultured using Advanced DMEM culture media containing 10% FBS, 1% P/S and 1% Glutamax (Gx) (HVSC culture media) in a T75 culture flask. Cells were cultured for 7 days with a starting seeding density of 0.5×10^5 cells/flask and culture medium was refreshed every 3 days. One day prior to the macrophage-conditioned media (MCM) stimulated migration experiment, HVSCs were stained with Cell tracker orange (CTO; Molecular probes, C34551) via a 30-minute incubation in HVSC culture media without FBS. Cells were washed twice with sterile PBS after which they were serum starved overnight in HVSC culture media containing 0.5% FBS.

3.2.2.1.1 Transwell gradient validation

To validate that the chemotactic gradient could be maintained for at least 4 hours (migration time) and consequently that migration of HVSCs occurred actively via chemotactic stimulation, a FitC-Inulin experiment was performed. FitC-inulin is a molecule with a fluorescent label (FitC). The amount of fluorescence through the FitC label can be used to determine concentration by including a standard curve with known concentrations in the fluorescence measurement.

A stock solution of 10mg/ml FitC-inulin was created by dissolving FitC-inulin in DMSO. FitC-inulin was diluted to concentrations ranging from 0.1mg/ml to 0.01mg/ml (in steps of 0.01mg/ml) to make a standard curve. At the start of the experiment, 2ml of 0.667 mg/ml FitC-inulin was pipetted in n=3 wells below the Transwells and 1.5ml of MiliQ was pipetted on top of each Transwell. At time points $t=10\text{min}, 30\text{min}, 60\text{min}, 120\text{min}, 180\text{min}$ and $t=210\text{min}$, 2x 20ul (Duplo) was taken from the top of each Transwell and collected in different Eppendorf tubes. These volumes were then further diluted 6 times by adding 100ul MiliQ.

After $t=210$ minutes, 100ul of each of the solutions collected at the different time points, together with 100ul of each standard curve concentration in Duplo, was pipetted in a black bottom 96 wells plate. Fluorescence values were determined using a plate reader device (Excitation= 485nm, emission=530nm) and corresponding concentration values were determined using the standard curve formula.

3.2.2.2 Modified Boyden chamber migration

After confirming that the chemotactic gradient could be maintained during migration time, cellular migration was assessed by using a modified Boyden Chamber assay (figure 2)²³. For each migration experiment, HVSCs were seeded on top of the Transwells (4.67 cm^2 surface area) using a seeding density of 0.25×10^5 cells/ cm^2 . Cells were let to adhere to the Transwell membranes for 3 hours, filling the top of the Transwells with 1.5ml and the bottom of the wells with 2ml of HVSC culture medium. After these 3 hours, media was removed and Transwells + wells were washed once with PBS. These cells were then stimulated to migrate for 4 hours through the Transwell membranes pores ($8\mu\text{m}$) by filling the bottom of the wells with 2ml of MCM obtained through biochemical or physically stimulated macrophage culture or with macrophage culture media containing either 20% FBS (positive control) or 10% FBS (negative control). For each migration experiment, one positive and negative control was included. The top of the Transwells themselves was filled with HVSC culture medium.

After this migration, media was removed from the Transwells + wells and both were washed twice with PBS. HVSCs on top of Transwells were fixed by incubating for 10 minutes at RT in a 3.7% formaldehyde solution. After fixing, the Transwell membranes were kept in PBS at 4°C until analysis.

3.3 Analyses

3.3.1 Migration

HVSC migration through the Transwell membranes in response to the different types of MCM was assessed from the location of cell nuclei and the formation of cell protrusions using confocal microscopy. To localize the cell nuclei, the membranes containing the HVSCs were stained with 4',6-diamidino-2-phenylindole (DAPI; Sigma, D9542; 2 ng/ml) for 5 minutes. Membranes were washed three times with PBS to remove DAPI and mounted onto glass slides using mowiol solution. For each sample, 4 separate z-stacks with a z distance of 1.5 µm in between each image, were made using the LEICA SP5X confocal microscope (Leica Microsystems CMS GmbH, Mannheim German) at a magnification of 20x. Number of cell nuclei (DAPI; pulsed diode laser 40 mHz, excitation 358 emission 461) and number of cell protrusions (plasma membrane protrusion at the leading edge; the initial step of migration²⁸ (CTO; white light laser, excitation 541 emission 565) were counted for each z-stack and the average over these 4 stacks was calculated.

As a measure for the number of migrating cells, the total number of cells on the top was divided by the number of protrusions depicted as protrusions/cell. This ratio is normalized to the negative control of the respective experiment to correct for experimental variability. Using this method, a cell is assumed to have either no protrusions (figure 3, A), one protrusion (Figure 3, B) or multiple protrusions (Figure 3, C). The number of cells on the bottom of the Transwell membrane are not counted due to insufficient cell number.

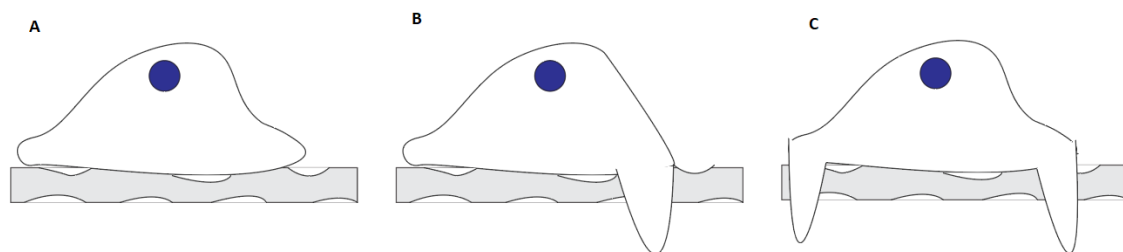


Figure 3, Schematic depicting HVSCs on top of Transwell membrane. HVSCs can have either: no protrusions (A), one protrusion (B) or two protrusions (C)

3.3.2 Gene expression

Cell-seeded scaffold strips were stored in cryovials containing 3 metal RNA-free beads. For each scaffold orientation, two cell-seeded scaffolds were pooled together in the same cryovial to ensure enough RNA could be obtained to perform qPCR.

These cell-seeded scaffolds were dismembrated (name) 3 times for 30 seconds at 3000 rpm and stored in liquid N₂ in between the shaking process to ensure scaffolds remained frozen. After scaffolds were pulverized, 600 µl RLT-buffer was added to each vial and scaffold RLT solution was transferred to a new Eppendorf tube. Samples were centrifuged at 4°C for 2 minutes and the supernatant was mixed 1:1 with ethanol solution (EtOH, Sigma).

The stored RLT-cell solution from the chemically stimulated PBMC culture was similarly mixed 1:1 with EtOH and similar protocols were followed for both solutions from this point onwards. RNA was isolated using the Qiagen RNeasy kit (Qiagen, Venlo, Netherlands), using the included

protocol. The final RNA concentration was determined using a spectrophotometer (Nanodrop, ND-1000, Isogen Life science, Ijsselstein) and RNA was stored at -20°C.

cDNA was created from 100ng of the isolated RNA using a Thermal Cycler (C1000 Touch, Bio-Rad, Hercules, CA, USA). For each cDNA sample, a control sample was made without the reverse transcriptase (-RT) to be used to check for genomic contamination.

cDNA was checked for genomic contamination by performing regular PCR using GAPDH primer as housekeeping gene and performing gel-electrophoreses. Primers relevant for macrophage polarization were used to perform real-time qPCR (CFX384 Touch Real-time PCR detection system, Bio-Rad, table 2) cDNA samples were diluted 100x in commercial water (ddH₂O).

Primer solutions for qPCR were created by mixing the diluted cDNA with the primers (500nM), ddH₂O and SYBR Green Super mix (Bio-Rad). ATP was included as reference genes for normalization of CT values.

For the qPCR itself, the following thermal protocol was used: 95 °C for 3 min, a cycle of each 95 °C for 20 s, 60 °C for 20 s and 72 °C for 30 s repeated 40 times, 95 °C for 1 min, 65 °C for 1 min and finally a melting curve measurement.

To visualize data results, the $\Delta\Delta C_t$ method was used. The CT values of samples were normalized to reference gene results and to either the unstimulated macrophage (M0, chemically stimulated experiment) or to statically cultured samples (strained samples, physically stimulated experiment).

Primer	Function	Primer sequence (5'-3')
MCP-1	Pro-inflammatory marker	FW: CAGCCAGATGCAATCAATGCC RV: TGGAATCCTGAACCCACTTCT
TNF-α	Pro-inflammatory marker	FW: GAGGCCAAGCCCTGGTATG RV: CGGGCCGATTGATCTCAGC
CCR7	Pro-inflammatory marker	FW: AAGCCTGGTTCCTCCCTATC RV: ATGGTCTTGAGCCTCTTGAAATA
TGF-β	Anti-inflammatory marker	FW: GCAACAATTCCTGGCGATACCTC RV: AGTTCTTCTCCGTGGAGCTGAAG
CD163	Anti-inflammatory marker	FW: CACTATGAAGAAGCCAAAATTACCT RV: AGAGAGAAAGTCCGAATCACAGA
CD206	Anti-inflammatory marker	FW: TGGGTTCTCTCTGGTTTCC RV: CAACATTTCTGAACAATCCTATCCA
IL-6	Migration marker	FW: ACTCACCTTTCAGAACGAATTG RV: GTCGAGGATGTACCGAATTTGT
IL-10	Migration marker/ Anti-inflammatory marker	FW: GACTTTAAGGGTTACCTGGGTTG RV: TCACATGCGCCTTGATGTCTG

Table 2, Primer names and sequences from 5' to 3' used for qPCR analysis

3.3.3 Immunofluorescence

At the start of the staining, cell seeded scaffold strips of each group were cut into 4 pieces (to reduce antibody volume needed), placed in 96 wells plates and permeabilized with 0.5% Triton X-100 for 15 minutes. These scaffold strips were washed once using PBS-Tween (0.1% Tween) and were blocked for 60 minutes using 5% Bovine Serum Albumin (BSA) in PBS-Tween, followed by an overnight incubation at 4 °C with the primary antibody mix (Table 3) in 1% BSA in PBS-Tween.

The following day, cell seeded scaffolds were washed three times for 5 minutes in PBS-Tween and afterward incubated in the secondary antibody mix (Table 3) in PBS-Tween for two hours. Cell seeded scaffold strips were washed twice for 5 minutes in PBS-Tween, followed by a 5-minute incubation with 1:500 DAPI (stock 1mg/ml) solution in PBS and washed 3 more times for 5 minutes with PBS-Tween. Samples were stored at 4 °C until microscopy.

Z-stacks of the bottom and top were made of each scaffold at 63x magnification using the Leica SP5x confocal microscope.

Using ImageJ software, the brightness in all frames of the z-stack images was increased and the background signal was reduced by removing all speckles with a diameter < 5 pixels. Images were converted to grayscale and a maximum intensity overlay was for each z-stack to visualize staining data results.

Marker	Function	Primary Ab	Dilution	Secondary Ab	Dilution
CD68	Pan-macrophage	Mouse anti-human IgG3,k	1:100	Alexa Fluor 488 Goat anti-mouse IgG3	1:200
CD64	M1 macrophage	Mouse anti-human IgG1	1:100	Alexa Fluor 647 Goat anti-mouse IgG1	1:300
CD163	M2 macrophage	Rabbit anti-human IgG	1:100	Alexa Fluor 555 Donkey anti-Rabbit IgG	1:300

Table 3, Primary and secondary antibody markers with the used immunoglobulin G(IgG), species and dilutions. M1 macrophage marker CD64, M2 macrophage marker = CD163, pan-macrophage marker = CD68.

3.4 Statistics

Data was plotted and analyzed using GraphPad PRISM software, and are depicted as mean +/- standard deviation. Data was assumed to not be nonparametric and a Kruskal-Wallis test was performed to analyze the data, using Dunns comparison as a post-hoc test to compare individual data columns.

4 Results

4.1 Scaffold characterization and strain validation

To determine fiber size and fiber orientation, images of both anisotropic and isotropic scaffold sheets were made using the ESEM (Figure 4AB, 5AB). By using a lower magnification, images depicted in figure 4B and figure 5B were made, these images were used as input for the Matlab script described by Haaften et al.²⁶, in order to determine the degree of anisotropy for each scaffold type. The output of Matlab script was depicted in an orientation histogram, showing along which degrees most fibers are aligned.

4.1.1 Scaffold sheet characterization

The average fiber diameter of the anisotropic scaffold sheet was determined by taking the average of 10 different fibers within image 4A, this diameter was calculated to be $3.62 \pm 0.37 \mu\text{m}$. The orientation histogram for the anisotropic scaffold sheet shows that most fibers are aligned along 120 and 300 degrees (Electrospinning collector at 90 degrees in the orientation histogram), indicating alignment along one direction (anisotropic alignment, figure 4C).

Using similar methods, the average fiber diameter in the isotropic scaffold sheet was measured to be $3.30 \pm 0.18 \mu\text{m}$ (figure 5A). The orientation histogram for the isotropic scaffold sheet shows no preference for fiber orientation since fibers are not aligned along specific directions (Figure 5C).

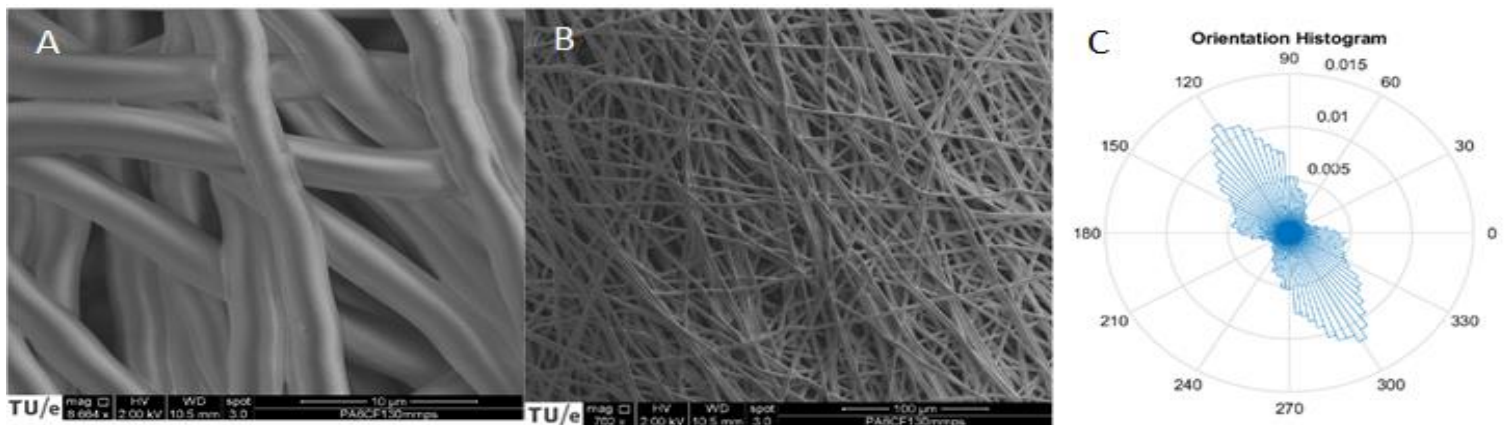


Figure 4, ESEM image of anisotropic scaffold sheet used to determine fiber diameter(A); ESEM image of anisotropic scaffold sheet used to determine degree of anisotropy(B); Orientation histogram of the created anisotropic scaffold created using Matlab(C)

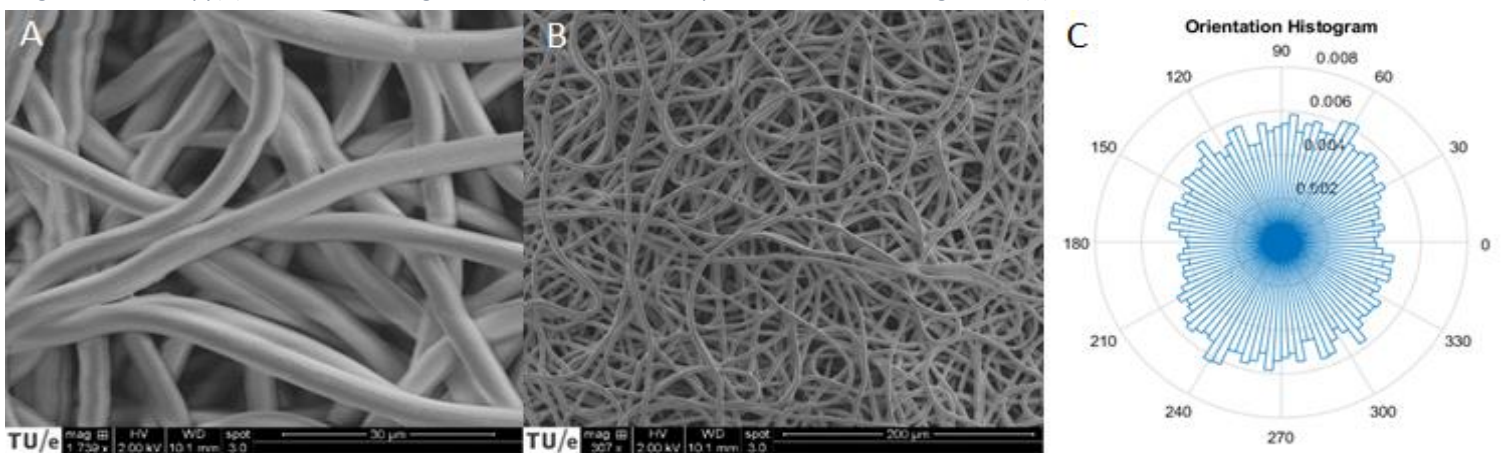


Figure 5, ESEM image of isotropic scaffold sheet used to determine fiber diameter(A); ESEM image of isotropic scaffold sheet used to determine degree of anisotropy(B); Orientation histogram of the created isotropic scaffold created using Matlab(C)

4.1.2 Scaffold strain validation

To determine if Flexcell software strain remained within the desired strain range (around 7% maximum strain) during physical conditioning, the maximum strain values of each cyclic stretch cycle at a device setting of '3%' strain was calculated for each fiber orientation. Results were fitted to a sine function in the format: $f(x) = a1*\sin(b1*x+c1)$. In this function, $a1$ is the amplitude of the sine function and therefore the maximum strain value exerted onto the different scaffold strips.

It can be observed that even though the stretch parameter on Flexcell device software is not altered, maximum strain seems to be increasing on a daily basis for each of the scaffold groups. Most scaffold orientations are within desired stretch range (~7%) by day 1.

Note that some graphs do not start at $t=0s$ and end at $t=1s$, this is the result of initial starting frame selection (Appendix A.1.2.) in combination with the fitting of the sine curve.

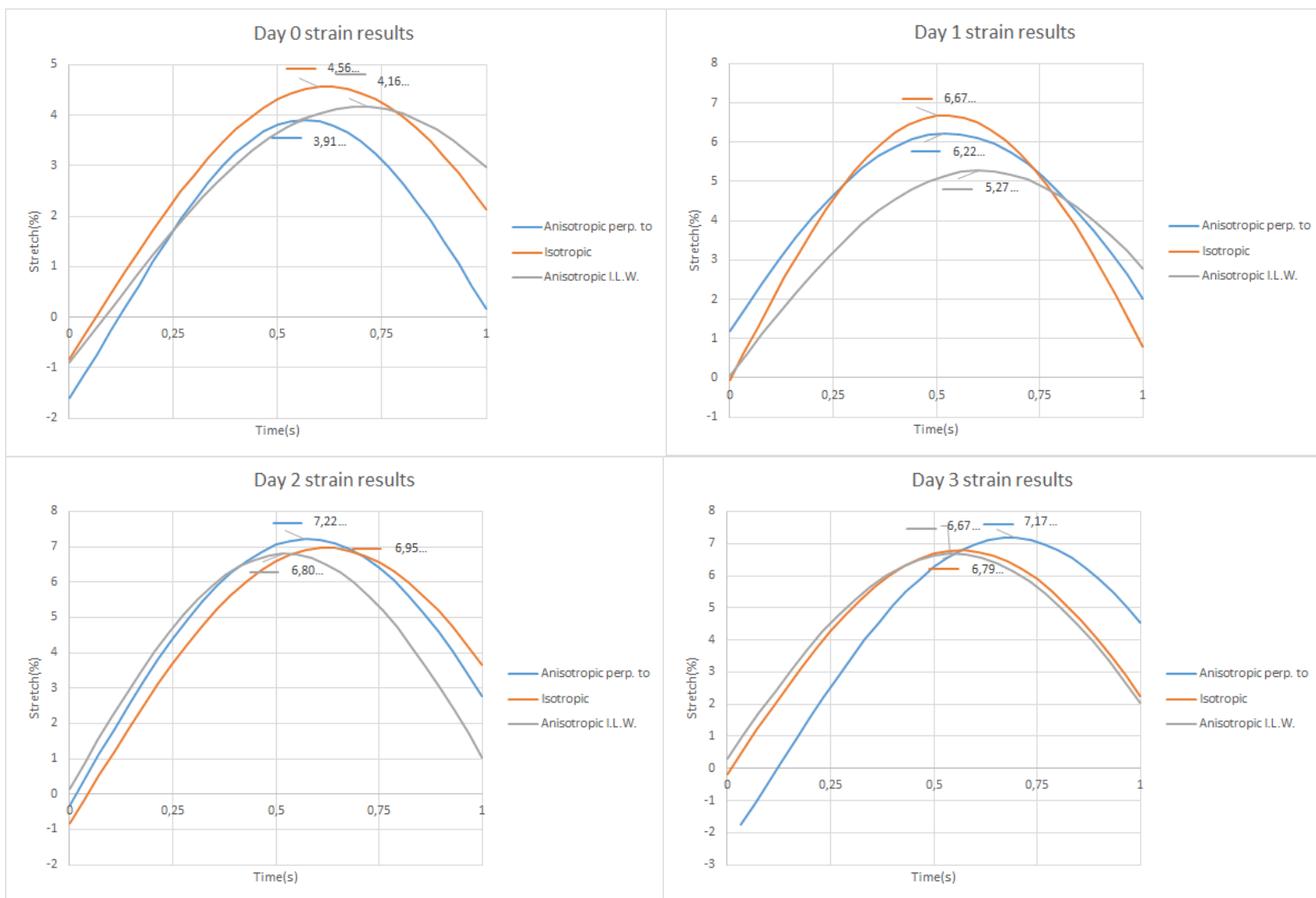


Figure 6, sine curve function $f(x) = a1*\sin(b1*x+c1)$, fitted to flexcell stretch result data. Flexcell stretch result data was obtained for each fiber orientation and maximum strain value (sine function amplitude), was included for each plot.

4.1.3 Transwell chemotactic gradient validation

To determine how long the created chemotactic gradient (through use of MCM) used to stimulate HVSC migration could be maintained, a FitC-inulin experiment was performed.

In this experiment, a known concentration of FitC-inulin was pipetted in the bottom of 6 wells plate, which diffused through a Transwell membrane.

Depicted in figure 6 are is the percentage of FitC-inulin present at the bottom and top of the well relative to the total amount of FitC-inulin present over time. The theoretical equilibrium concentration of FitC-inulin is depicted by the dashed line at 50% FitC amount (figure 6).

It can be observed that the FitC-inulin molecule seems to diffuse gradually from the bottom of the well to on top of the Transwell. At $t=210$ minutes, FitC-inulin has yet to reach complete equilibrium indicating that a chemotactic gradient can be maintained for at least 3.5 hours. Based on this information, it was decided to let the cells migrate for 4 hours, to ensure active migration of HVSCs.

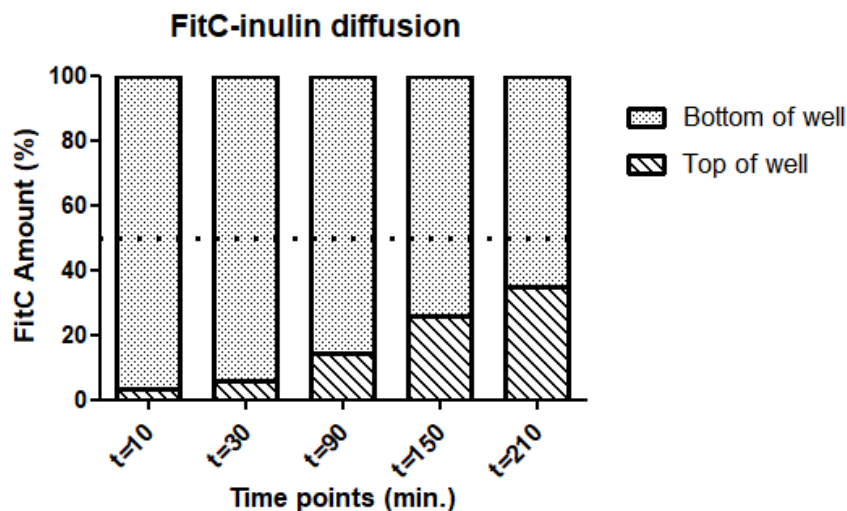


Figure 6, Amount of FitC-inulin present in the bottom of the well in relation to the amount present on top of the Transwell membrane at different points over time. The dashed line represents the FitC-inulin being in total equilibrium between bottom and top of the well

4.2 Biochemically stimulated macrophages

4.2.1 Phenotypical characterization- qPCR

To determine if polarization towards the desired phenotype had occurred for the biochemically stimulated PBMC culture, a qPCR analysis was performed.

Results of this qPCR analysis are depicted in figure 7. In this figure, fold change values of pro- and anti-inflammatory macrophage markers of the biochemically stimulated PBMC culture are plotted. Pro-inflammatory markers show an increase in fold change values compared to unstimulated (M0) and anti-inflammatory(M2) macrophages.

Anti-inflammatory macrophage markers CD-163 and CD206 seem to have an increase fold change compared to both M0 and M2 markers, whereas TGF- β and IL-10 markers do not differ much between M1 and M2 macrophage groups.

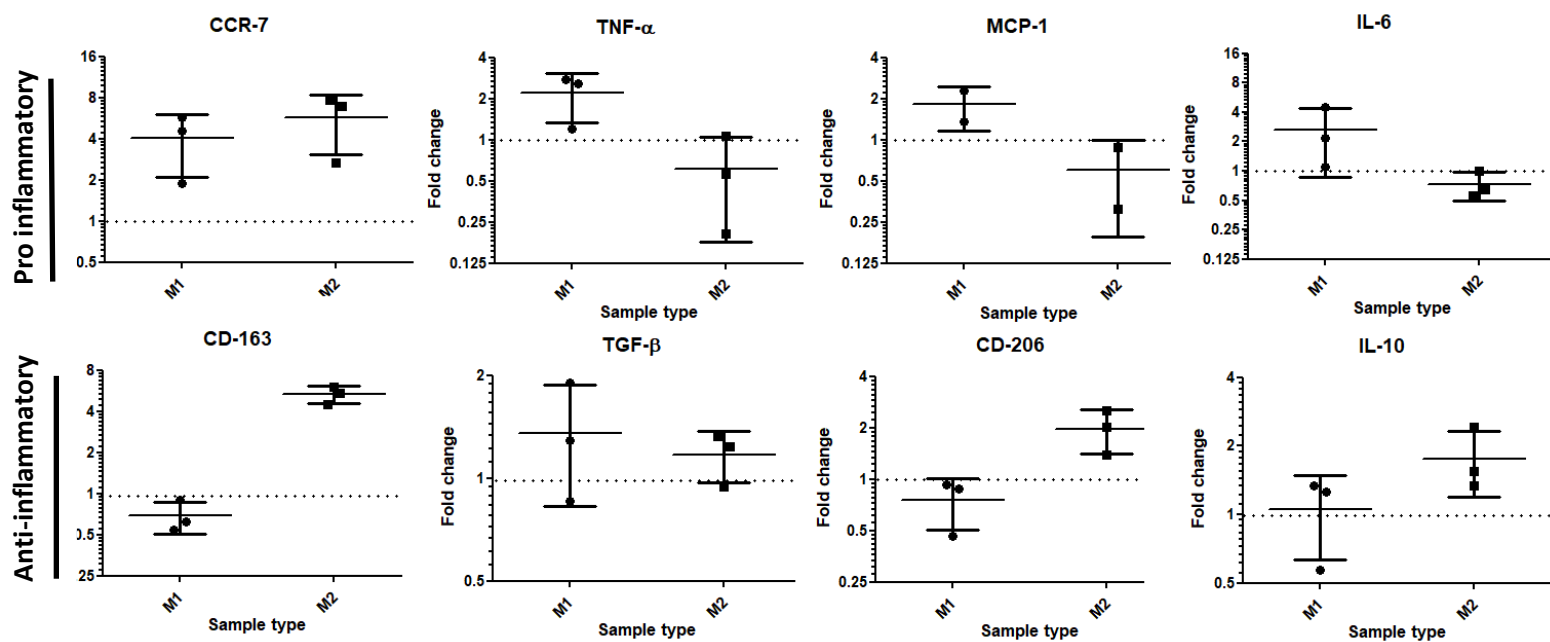


Figure 7, qPCR fold change values from chemically stimulated PBMC culture; Top row consists of pro-inflammatory markers, bottom row consists of anti-inflammatory markers. The dashed line represents the unstimulated macrophages (M0)

4.2.2 HVSC migration- biochemically stimulated MCM

The difference in HVSC migration in response to MCM obtained through the biochemically stimulated PBMC cultures was compared by plotting the amount of protrusions/cell for each of the three groups (M0, M1, M2; Figure 8).

It can be observed that M1 MCM seems to induce the most protrusions/cell and that it significantly differs from the positive control value. However, there are no significant differences between M1 MCM and other MCM types. Moreover, it appears that all MCM groups have an increased response compared to positive control values.

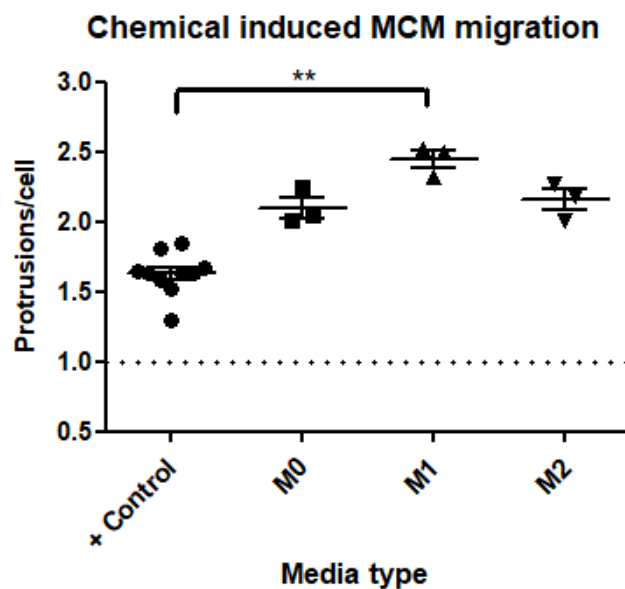


Figure 8, Amount of protrusions/cell normalized to the negative control, induced by MCM obtained from biochemically stimulated PBMC cultures. Depicted on the x-axis are the different MCM types (and positive control) used to stimulate migration, M0=unstimulated, M1 = stimulated by IFN- γ and M2= stimulated by IL-4. ** represents statistical difference ($p=0.002$).

4.3 Physically stimulated macrophages

4.3.1 Phenotypical characterization- qPCR

Similarly, to determine the phenotype of the physically stimulated PBMC cultures, a qPCR analysis was performed. Due to RNA loss, only qPCR values of the isotropic scaffold sheet orientation are available (figure 9). CT values of the strained PBMC culture were normalized to their static counterpart (figure 9, dashed line).

Results show a decrease in fold change for most pro- and anti-inflammatory markers compared to statically cultured counterpart. Fold change values for marker IL-6 show a big increase in IL-6 expression for the strained isotropic scaffold PBMC compared static culture (fold change > 5).

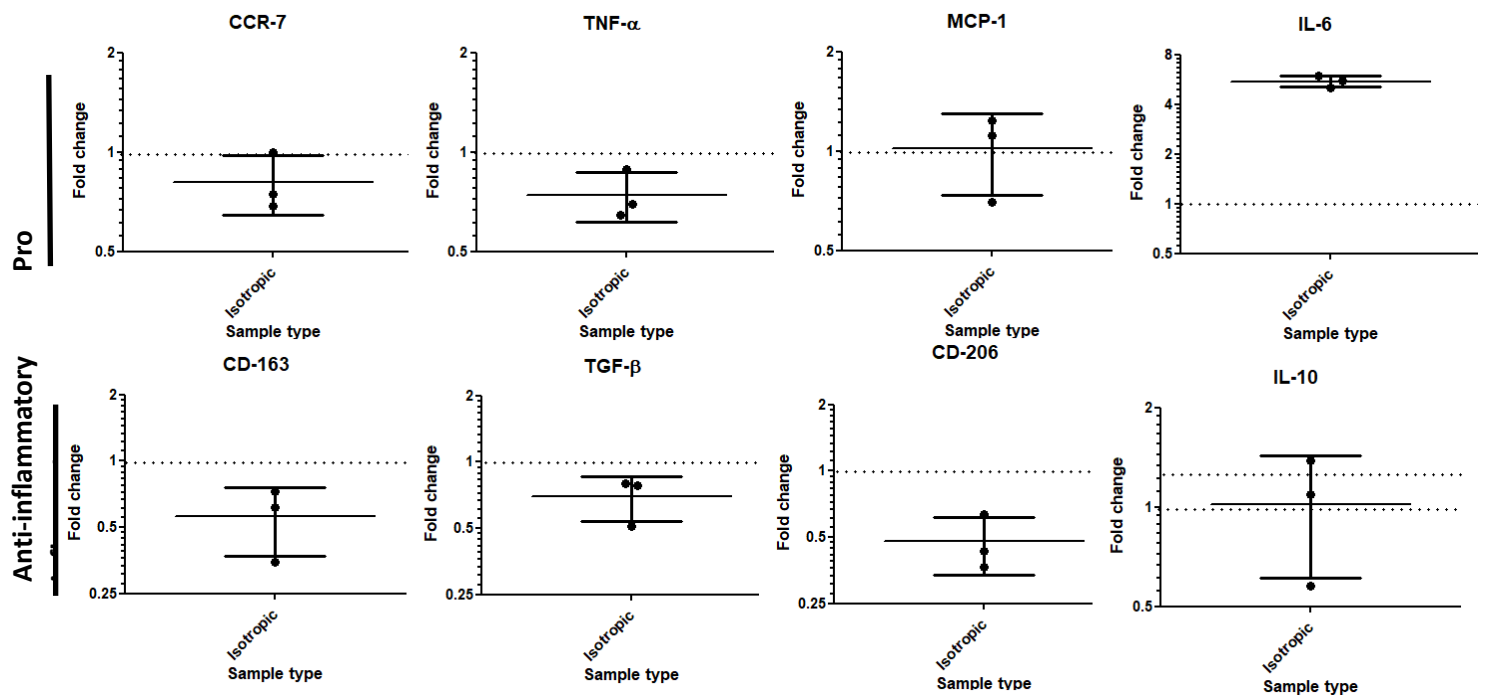


Figure 9, qPCR fold change values from physically stimulated PBMC culture; Top row consists of pro-inflammatory markers, bottom row consists of anti-inflammatory markers. The dashed line represents PBMCs cultured statically on the isotropic scaffolds

4.3.2 Phenotypical characterization- Immunofluorescence

To further confirm macrophage phenotype for the physically conditioned PBMC cultures, antibody staining was performed on all scaffold sheets of all orientations. Representative figures of combined antibody and DAPI staining on statically and strained PBMCs cultures are depicted below in figures 10 and 11.

Results of DAPI staining show cell infiltration throughout scaffolds in both static and strained culture groups. CD68 (Pan macrophage marker) staining is present throughout all scaffolds in both static and strained groups, indicating the presence of a cell with monocyte lineage.

Statically cultured groups anisotropic I.L.W. and isotropic show little expression of CD68 and CD64 and more CD163 expression, indicating more M2 macrophage presence. Many cells co-express both M1 and M2 marker, indicated by a yellow color in the composite image.

Cyclically strained groups seem to have overall equal amounts of CD64 expression compared to static sample with the exception of strained scaffolds with isotropic orientation, showing increased CD64 expression.

It can also be observed that throughout all cyclically cultured groups, CD163 expression is vastly decreased, indicating an increase in M1/M2 ratio.

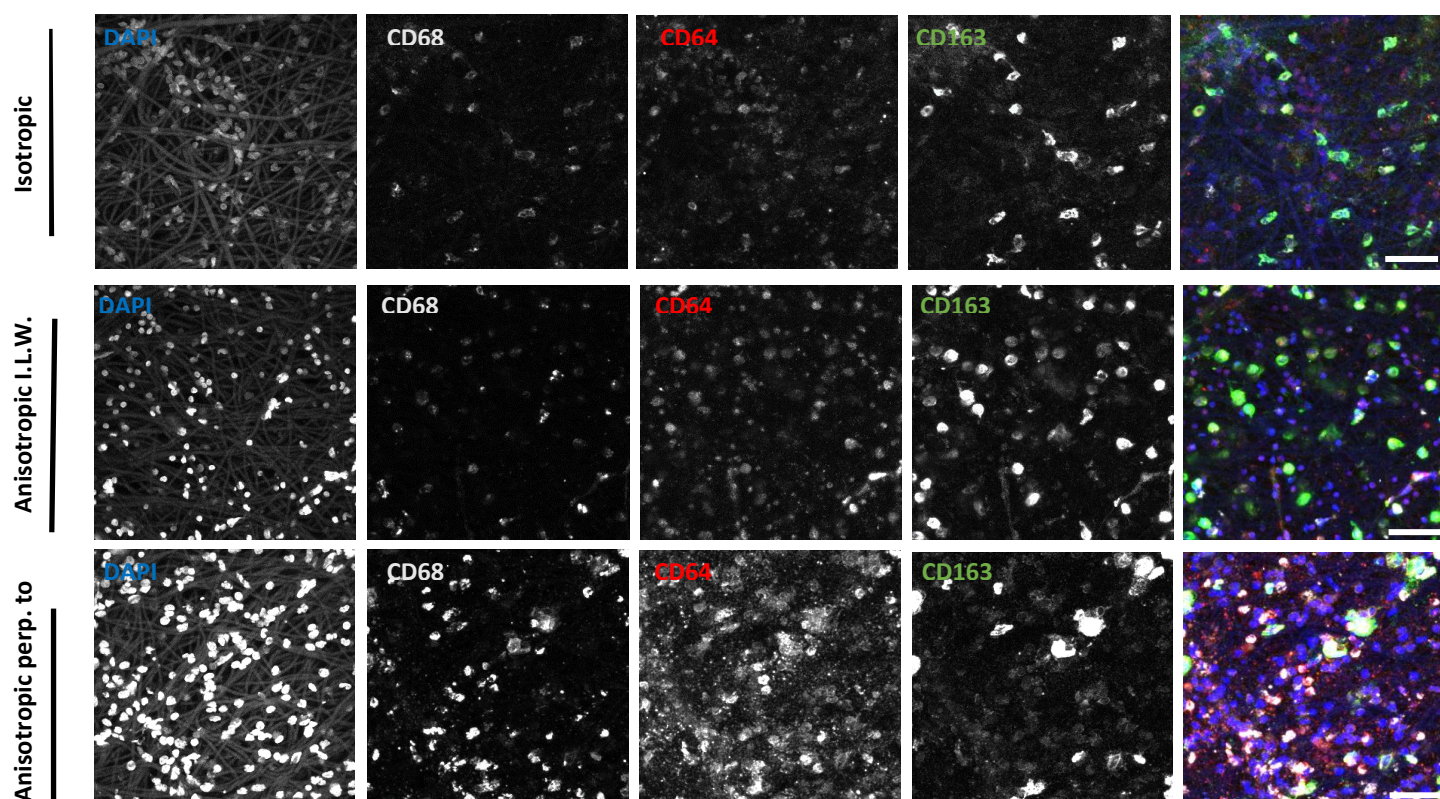


Figure 10, Macrophages polarization in response to 3 day static culture on scaffolds with different degree of anisotropy. Each scaffold group was stained and the letters in which staining is written indicate color in composite image. Staining includes DAPI (nucleus, blue), CD68(Pan-macrophage, gray), CD64 (M1, red) and CD163 (M2, green). Scale bar in combined image indicates 50 μ m.

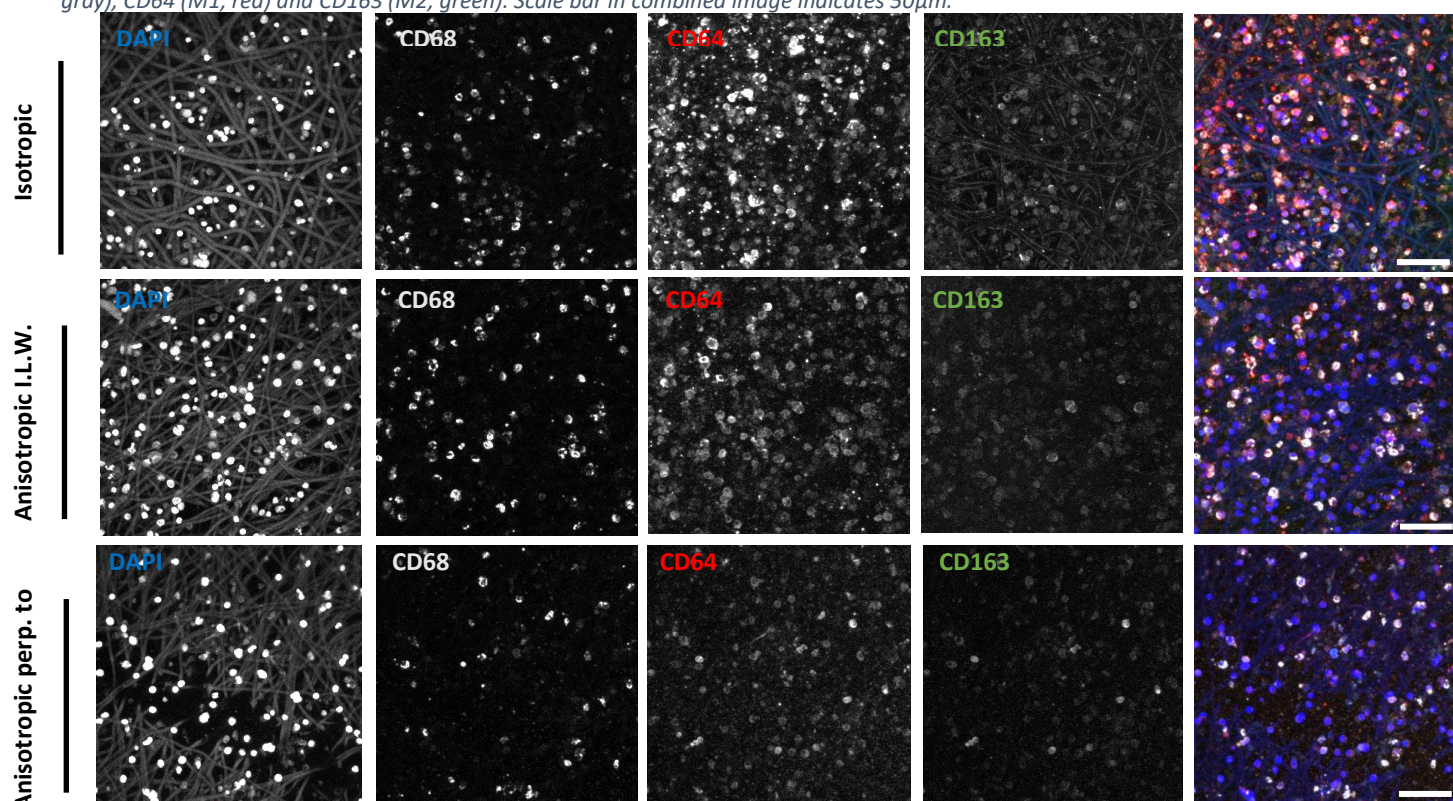


Figure 11, Macrophages polarization in response to 3 day cyclically strained culture on scaffolds with different degree of anisotropy. Each scaffold group was stained and the letters in which staining is written indicate color in composite image. Staining includes DAPI (nucleus, blue), CD68(Pan-macrophage, gray), CD64 (M1, red) and CD163 (M2, green). Scale bar in combined image indicates 50 μ m.

4.3.3 HVSC migration- Physically stimulated MCM

The effect of physical stimulation through fiber orientation and the combined effect of fiber orientation and cyclic strain on MCM and consequently HVSC migration was assessed by separately plotting static and cyclically strained groups (figure 12AB).

The effect of cyclic straining on HVSC migration was in turn assessed by plotting static and strained scaffolds of similar orientation together with the positive control values (figure 13).

HVSC migration results obtained through static PBMC culture on different fiber orientations (figure 12A) show no significant differences between any fiber alignments and the positive control, yet a slight non-significant decrease in number of protrusions/cell seems to be observed for scaffolds with orientation anisotropic in line with strain (Aniso. I.L.W.)

The effect of fiber alignment obtained through strained PBMC culture on HVSC migration can be observed in figure 12B. It can be observed that there seems to be an increase in the number of HVSC protrusions/cell compared to positive controls, yet no significant differences are present.

Straining of isotopically aligned scaffold groups seems to have minimal effects on the number of HVSC protrusions/cell, yet donor variance seems to play a role in the strained groups here (Figure 13A). The effect of cyclic strain on both anisotropically aligned groups (Aniso I.L.W. and perp. to, figure 13B, C) seem to cause an increase in the number of protrusions/cell, with a significant increase in number of protrusions/cell for scaffolds with orientation anisotropic in line with (Figure 13C).

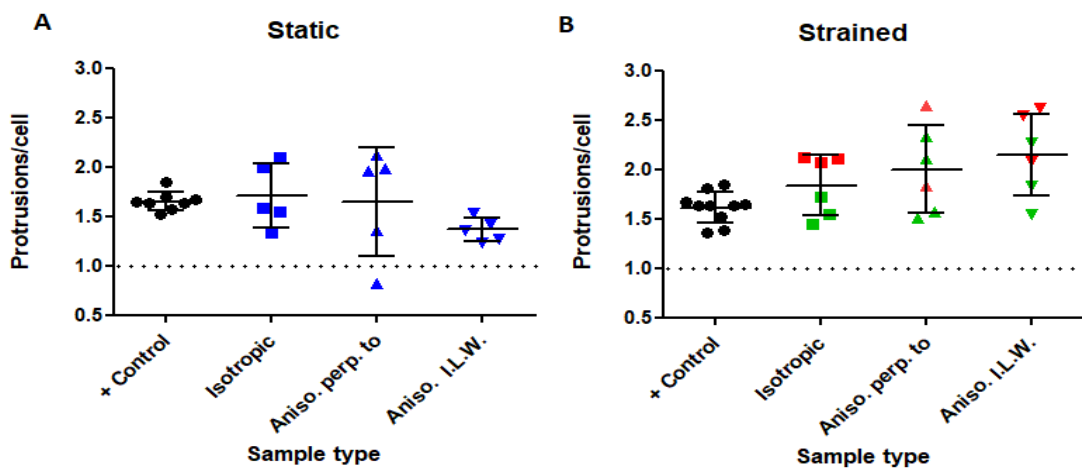


Figure 12, HVSC migration quantified as number of protrusions/cell, stimulated by MCM obtained through physically stimulated PBMC culture, PBMCs were cultured on scaffolds with different degrees of anisotropy and either statically cultured (A) or cultured exposed to cyclic strain (B). Different colors indicate a difference in PBMC donor.

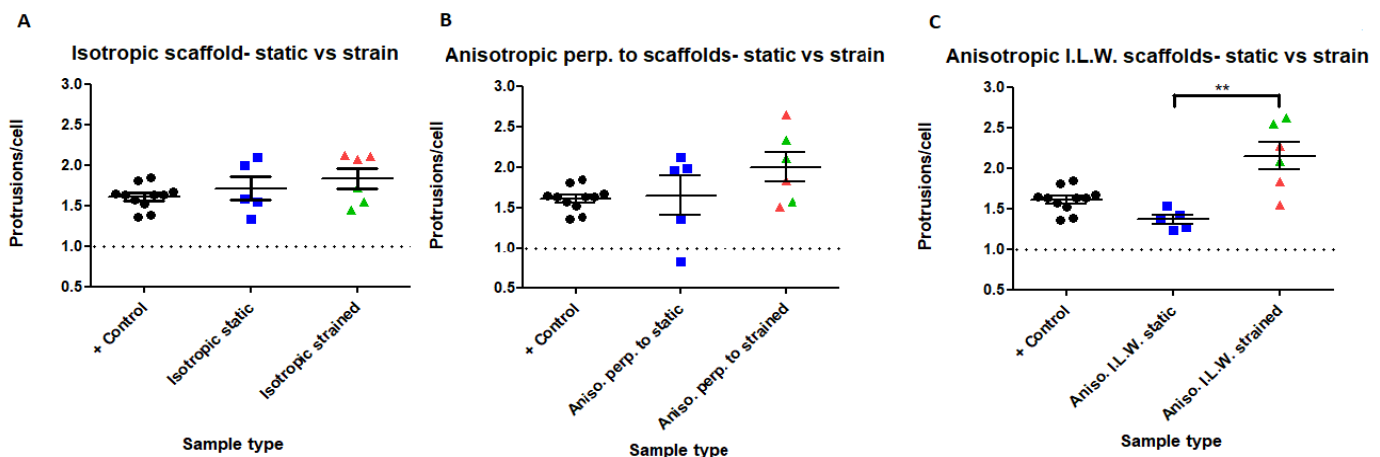


Figure 13, HVSC migration described by number of protrusions/cell, stimulated by MCM obtained through physically stimulated PBMC culture. Statically and cyclically strained cell seeded scaffolds with similar fiber orientation were plotted together. Fiber orientations were either isotropic (A), Anisotropic perpendicular to (B) or anisotropic in line with (C). Different PBMC donor are depicted through difference in color. ** indicates a statistical difference ($P=0.0021$)

5 Discussion

The biggest problem of AVGs, used to create blood flow access for end stage renal disease (ESRD) patients, is the occurrence of neo-intimal hyperplasia leading to venous stenosis. The implantation of any material (like the AVGs) in the human body causes a foreign body response (FBR) in which macrophages are key players. Macrophages interact with many cell types, including myofibroblasts and SMCs, influencing the process of neo-intimal hyperplasia.^{15,21} Macrophages are a plastic cell type whose phenotype and therefore function can be steered to either pro-inflammatory (M1) or anti-inflammatory (M2). This phenotype can be altered by factors such as fiber alignment, cyclic strain or chemical stimulation via soluble factors.

The goal of this research was to investigate the effects of macrophage polarization under the influence of biochemical or physical factors (i.e. cyclic strain and scaffold microarchitecture) on the migration of myofibroblasts. Instead of using a pure population of macrophages, peripheral blood mononuclear cells (PBMCs) were stimulated chemically via IL-4 (M2) or IFN- γ (M1) or physically by seeding them on scaffolds with different degrees of anisotropy and cyclically straining these.

It was hypothesized that macrophages with anti-inflammatory characteristics (M2) induce the most HVSC migration compared to unstimulated or M1 stimulated macrophages.

Successful macrophage polarization of the biochemically stimulated PBMC culture was verified through qPCR analysis. Results for the IFN- γ stimulated PBMC culture (M1-macrophage culture), showed that M1 related genes MCP-1 and TNF- α were upregulated compared to M2 and M0 cultures. Similarly, results for the IL-4 stimulated PBMC culture showed upregulation of genes CD-163 and CD206 (related to M2 macrophages) compared to M1 and M0 polarized groups. These trends were however not visible for every M1 or M2 related gene. However, since macrophages have many sub-types and these sometimes overlap, it is expected that not every marker related to the general M1 or M2 paradigm is upregulated.^{11,12}

It is more difficult to define phenotype for the physically stimulated PBMC cultures since only qPCR results are available for scaffolds with isotropic fiber orientation. The gene expression results for macrophages cultured on isotopically aligned scaffolds showed an overall downregulation for most M1 and M2 genes as a result of the cyclic straining. Interestingly, the migration marker IL-6 was highly upregulated (fold change >5) marker compared its statically cultured counterpart. IL-6 is a pro-inflammatory cytokine that can be produced by both M1 and M2b macrophages, providing little knowledge regarding macrophage polarization.²⁹

Immunofluorescence results for fiber orientations anisotropic I.L.W. and isotropic, of the physically stimulated, static PBMC cultures, showed an overall increased signal of M2 marker CD163 compared to M1 marker CD64. Indicating more M2-macrophage presence under static culture conditions. Under static culture conditions, scaffold orientation anisotropic perp. to showed more M1-marker expression than orientation anisotropic I.L.W. , which was unexpected since no strain was exerted and these scaffold orientations were cut out of the same sheet. This observation could be the result of a difference in sheet thickness.

Cyclically strained cell seeded scaffolds, showed an overall decrease in CD163 (M2 marker) expression compared to their static counterparts, suggesting an increase in M1/M2 ratio. It was unexpected that a decrease in M2 macrophages was already seen at physiological strain levels (7%) here since it has been previously shown that this decrease only occurs at high strain levels (>12%).¹³

The experimental results for the biochemically stimulated PBMC cultures suggest that not M2 macrophages (as hypothesized in the introduction), but M1 macrophages seem to cause an increased number of protrusions/cell. Results between the different macrophage phenotypes were, however, not significant, making it difficult to draw an accurate conclusion.

MCM derived from M1 macrophage cultures did show a significant increase in number of HVSC protrusions/cell compared to positive control groups, indicating an increased amount of migration.^{28,30}

Physically stimulated MCM migration experiment results showed that cyclic strain seemed to cause an overall increase in the number of HVSC protrusions/cell cyclic strain compared to unstrained groups (static). However, only a significant difference in number of HVSC protrusions/cell could be seen when comparing static and cyclically strained anisotropic I.L.W. groups.

This increase in HVSC protrusions/cell for the group anisotropic I.L.W. was previously hypothesized in the introduction. However, this hypothesis was based on the premise that cyclic straining at 7%, as well as anisotropic fiber alignment, would cause an increase in M2 macrophage polarization.^{13,20} On the contrary, a decrease in M2 marker was seen in immunological results for all strained groups.

These results, in turn, seem to agree with the findings of the biochemically stimulated MCM migration experiment, where M1 macrophages seemed to cause the most migration. Due to lack of qPCR data for the anisotropic fiber alignments, macrophage phenotype and consequently the statement that M1-macrophages seem to cause more HVSC migration, cannot be accurately confirmed.

In similar research by Lavin et al.³¹ regarding neointimal hyperplasia, murine M1 conditioned MCM was described to cause an increase in VSMC migration in 2D, which is in agreement with the alleged findings of this research.

In a different research paper by Verma et al.³², IL-10 knockout mice displayed enhanced neo-intimal growth which was blunted by exogenous administration of this cytokine. IL-10 has been related to M2-macrophage phenotype, suggesting the relevance of M2 macrophages in preventing neo-intimal hyperplasia.

However, there is little direct research available regarding the phenotype of macrophages on the process of neo-intimal hyperplasia, yet research regarding cytokines directly affecting migration of fibroblasts and SMCs is widely available. Cytokines like IL-1, IFN γ , IL-1 β , IL-6, TGF β 1, TNF- α , IL-22, IL-19, IL-4 and IL-10 have all been shown to affect the migration of either fibroblasts or SMCs, describing possible involvement in the process of neo-intimal hyperplasia and highlighting the importance of including these factors in future research.³³⁻³⁷

This study also has several limitations. First of all, instead of seeding a pure monocyte population, PBMCs, which also contain lymphocytes, were used. Therefore, the assumption has to be made that cell types besides macrophages present in the PBMC population are discarded after the 1st washing step in each experiment since macrophages are the only cell type capable of adhering to surfaces.³⁸ The results of the physically cultured PBMC migration experiment show a large standard deviation between groups of similar scaffold orientations. This can be attributed to donor variation and experiment reproducibility. The PBMCs that were used are primary human immune cells which are dependent on host conditions like diet or genetics.³⁹ Donor variability further hinders the accurate comparison of static and strained migration experiments, since different PBMC donors have been used.

Experiment reproducibility could have been affected by slight differences in scaffold thickness, width or length, causing actual strain to vary between scaffold strips.

The quantification of both the number of protrusions and the number of cells is affected by human error since this was all executed manually.

On top of this, in this research migration is quantified by the number of protrusions/cell. Even though cell migration can be characterized by cellular budding and protrusion formation^{30,40}, there is no guarantee that the number of protrusions/cell directly relates to the amount of migration.

Improvements to the research outcome can be made by increasing sample size for MCM obtained through chemically stimulated PBMC culture.

Another set of immunological staining of different markers also expressed by M1 and M2 macrophage phenotypes will provide more accurate information regarding macrophage polarization since macrophages are a blend of phenotypes, rather than a strict division between M1 and M2.

For future research purposes, it would be beneficial to exclude the human aspect of migration quantification by using computer-assisted image recognition and analysis methods.

Decreasing chemoattractant diffusion speed (for example by coating the Transwells) and as a result, prolong migration experiment duration will enable cells to be quantitatively measured at the bottom of the wells.

An experiment measuring the migration response of HVSCs to an array of macrophage-expressed cytokines can also provide further insight in determining the biggest contributors to neo-intimal hyperplasia.

Overall the findings of this research and previously mentioned literature, suggest that M1 macrophages seem to have a greater influence on the migration of myofibroblasts than M2 macrophages. This highlights the importance of promoting M2 macrophage polarization when designing in-situ TE AVGs in order to prevent neo-intimal hyperplasia formation, further research is necessary to accurately confirm this statement.

6 Conclusion

In this study, the effect of factors affecting macrophage phenotype, such as chemical stimuli, fiber alignment and cyclic stretch, on the migration of HVSCs was researched, in order to elucidate the mechanisms underlying neo-intimal hyperplasia.

Comparison of MCM collected by seeding PBMCs seeded on different scaffold fiber orientations showed no significant effect on the migration of HVSCs in both statically and strained culture groups. Cyclic straining at 7% seemed to play a bigger role, causing an increase in HVSC migration compared to statically cultured groups. Immunology results for cyclically strained groups showed an overall decrease in CD163 (M2 marker) expression. On top of this, qPCR results for isotopically strained scaffold groups showed an overall decrease in both M1 and M2 markers, suggesting an upregulated HVSC migration response due to an increase in M1/M2 ratio.

Moreover, biochemically induced M1 (via IFN- γ) MCM seemed to demonstrate an increased HVSC migration response compared to the positive control (significant), M0 MCM (unstimulated macrophages, non-significant) and M2 MCM (IL-4 induced, non-significant).

Overall, the results propose M1 macrophages to play a bigger role in causing neo-intimal hyperplasia compared to other phenotypes, yet further experiments are needed to confirm these observed effects.

7 References

1. Feiten en cijfers - Nierstichting. Available at: <https://www.nierstichting.nl/leven-met-een-nierziekte/feiten-en-cijfers/>. (Accessed: 29th April 2019)
2. End Stage Renal Disease in the United States | National Kidney Foundation. (2016). Available at: <https://www.kidney.org/news/newsroom/factsheets/End-Stage-Renal-Disease-in-the-US>. (Accessed: 29th April 2019)
3. Global Facts: About Kidney Disease | National Kidney Foundation. (2015). Available at: <https://www.kidney.org/kidneydisease/global-facts-about-kidney-disease>. (Accessed: 29th April 2019)
4. National kidney foundation. Hemodialysis | National Kidney Foundation. (2015). Available at: <https://www.kidney.org/atoz/content/hemodialysis>. (Accessed: 29th April 2019)
5. Rosas, S. E. & Feldman, H. I. Synthetic vascular hemodialysis access versus native arteriovenous fistula: a cost-utility analysis. *Ann. Surg.* **255**, 181–6 (2012).
6. Gayle Romancito. Hemodialysis | NIDDK. (2018). Available at: <https://www.niddk.nih.gov/health-information/kidney-disease/kidney-failure/hemodialysis>. (Accessed: 29th April 2019)
7. Peck, M. K. *et al.* New Biological Solutions for Hemodialysis Access. *J. Vasc. Access* **12**, 185–192 (2011).
8. Shi, Z.-D. & Tarbell, J. M. Fluid Flow Mechanotransduction in Vascular Smooth Muscle Cells and Fibroblasts. *Ann. Biomed. Eng.* **39**, 1608–1619 (2011).
9. Wissing, T. B., Bonito, V., Bouten, C. V. C. & Smits, A. I. P. M. Biomaterial-driven in situ cardiovascular tissue engineering—a multi-disciplinary perspective. *npj Regen. Med.* **2**, 18 (2017).
10. Anderson, J. M., Rodriguez, A. & Chang, D. T. Foreign body reaction to biomaterials. *Semin. Immunol.* **20**, 86–100 (2008).
11. Mosser, D. M. & Edwards, J. P. Exploring the full spectrum of macrophage activation. *Nat. Rev. Immunol.* **8**, 958–969 (2008).
12. Martinez, F. O. & Gordon, S. The M1 and M2 paradigm of macrophage activation: time for reassessment. *F1000Prime Rep.* **6**, 13 (2014).
13. Ballotta, V., Driessen-Mol, A., Bouten, C. V. C. & Baaijens, F. P. T. Strain-dependent modulation of macrophage polarization within scaffolds. *Biomaterials* **35**, 4919–4928 (2014).
14. Liu, X., Peyton, K. J. & Durante, W. Physiological cyclic strain promotes endothelial cell survival via the induction of heme oxygenase-1. *Am. J. Physiol. - Hear. Circ. Physiol.* **304**, H1634 (2013).
15. Holt, D. J., Chamberlain, L. M. & Grainger, D. W. Cell–cell signaling in co-cultures of macrophages and fibroblasts. *Biomaterials* **31**, 9382–9394 (2010).
16. Oya, K., Sakamoto, N. & Sato, M. Hypoxia suppresses stretch-induced elongation and orientation of macrophages. *Biomed. Mater. Eng.* **23**, 463–471 (2013).
17. Brown, B. N. *et al.* Macrophage phenotype as a predictor of constructive remodeling following the implantation of biologically derived surgical mesh materials. *Acta Biomater.* **8**, 978–987 (2012).

18. Wang, Z. *et al.* The effect of thick fibers and large pores of electrospun poly(ϵ -caprolactone) vascular grafts on macrophage polarization and arterial regeneration. *Biomaterials* **35**, 5700–5710 (2014).
19. Luu, T. U., Gott, S. C., Woo, B. W. K., Rao, M. P. & Liu, W. F. Micro- and Nanopatterned Topographical Cues for Regulating Macrophage Cell Shape and Phenotype. *ACS Appl. Mater. Interfaces* **7**, 28665–28672 (2015).
20. Garg, K., Pullen, N. A., Oskeritzian, C. A., Ryan, J. J. & Bowlin, G. L. Macrophage functional polarization (M1/M2) in response to varying fiber and pore dimensions of electrospun scaffolds. *Biomaterials* **34**, 4439–51 (2013).
21. Van Linthout, S., Miteva, K. & Tschöpe, C. Crosstalk between fibroblasts and inflammatory cells. *Cardiovasc. Res.* **102**, 258–269 (2014).
22. Battiston, K. G., Ouyang, B., Labow, R. S., Simmons, C. A. & Santerre, J. P. Monocyte/macrophage cytokine activity regulates vascular smooth muscle cell function within a degradable polyurethane scaffold. *Acta Biomater.* **10**, 1146–1155 (2014).
23. Chen, H.-C. Boyden Chamber Assay. in *Cell Migration* 015–022 (Humana Press, 2005). doi:10.1385/1-59259-860-9:015
24. Schnell, A. *et al.* Optimal Cell Source for Cardiovascular Tissue Engineering: Venous vs. Aortic Human Myofibroblasts. *Thorac. Cardiovasc. Surg.* **49**, 221–225 (2001).
25. Brugmans, M. C. P. The interplay between biomaterial degradation and tissue properties : relevance for in situ cardiovascular tissue engineering. (2015).
26. van Haaften, E. E. *et al.* Decoupling the Effect of Shear Stress and Stretch on Tissue Growth and Remodeling in a Vascular Graft. *Tissue Eng. Part C Methods* **24**, 418–429 (2018).
27. Neggers, J., Blaysat, B., Hoefnagels, J. P. M. & Geers, M. G. D. On image gradients in digital image correlation. *Int. J. Numer. Methods Eng.* **105**, 243–260 (2016).
28. Barry, D. J., Durkin, C. H., Abella, J. V & Way, M. Open source software for quantification of cell migration, protrusions, and fluorescence intensities. *J. Cell Biol.* **209**, 163–80 (2015).
29. Bio rad. *Macrophage polarization Mini Review.* (2015).
30. Xue, F., Janzen, D. M. & Knecht, D. A. Contribution of Filopodia to Cell Migration: A Mechanical Link between Protrusion and Contraction. *Int. J. Cell Biol.* **2010**, (2010).
31. Lavin, B. *et al.* Nitric Oxide Prevents Aortic Neointimal Hyperplasia by Controlling Macrophage Polarization. *Arterioscler. Thromb. Vasc. Biol.* **34**, 1739–1746 (2014).
32. Verma, S. K. *et al.* IL-10 Accelerates Re-Endothelialization and Inhibits Post-Injury Intimal Hyperplasia following Carotid Artery Denudation. *PLoS One* **11**, e0147615 (2016).
33. Sprague, A. H. & Khalil, R. A. Inflammatory cytokines in vascular dysfunction and vascular disease. *Biochem. Pharmacol.* **78**, 539–52 (2009).
34. Postlethwaite, A. E. & Seyer, J. M. Fibroblast chemotaxis induction by human recombinant interleukin-4. Identification by synthetic peptide analysis of two chemotactic domains residing in amino acid sequences 70-88 and 89-122. *J. Clin. Invest.* **87**, 2147–52 (1991).
35. King, A., Balaji, S., Le, L. D., Crombleholme, T. M. & Keswani, S. G. Regenerative Wound Healing: The Role of Interleukin-10. *Adv. wound care* **3**, 315–323 (2014).
36. Shi, H. *et al.* Metabolites of Hypoxic Cardiomyocytes Induce the Migration of Cardiac

- Fibroblasts. *Cell. Physiol. Biochem.* **41**, 413–421 (2017).
37. Fatkhullina, A. R., Peshkova, I. O. & Koltsova, E. K. The Role of Cytokines in the Development of Atherosclerosis. *Biochemistry. (Mosc).* **81**, 1358–1370 (2016).
 38. Tsang, M., Gantchev, J., Ghazawi, F. M. & Litvinov, I. V. Protocol for adhesion and immunostaining of lymphocytes and other non-adherent cells in culture. *Biotechniques* **63**, 230–233 (2017).
 39. Huang, E. & Wells, C. A. The Ground State of Innate Immune Responsiveness Is Determined at the Interface of Genetic, Epigenetic, and Environmental Influences. *J. Immunol.* **193**, 13–19 (2014).
 40. Barry, D. J., Durkin, C. H., Abella, J. V. & Way, M. Open source software for quantification of cell migration, protrusions, and fluorescence intensities. *J. Cell Biol.* **209**, 163 (2015).

8 Appendices

A.1. Matlab scripts

A.1.1. Gdicpost_PO

Post-processing script

```
%% Post-processing of GDIC GUI version

% Pim Oomen,
% Updated: 2015/12/02

% N.B. In the Results section of the GDIC GUI, select Green-Lagrange
% strain as output and save data using 'Info'>'Save guidata to D'

%% User input

% File properties
fDir = 'documents/gdic flexcell package/data/'; % Working directory
wkspName = 'day 2 iso exp 3'; % Workspace (generated in
this file) name

% Plot/Video parameters (not affecting solution)
vidSwitch = true; % Generate video (time-consuming)
vidFigSwitch = true; % Store video frames as images (time-consuming)
nArrows = 1; % Number of arrows in video & images
border = 0; % Exclude border region (px)
frameRate = 10; % Frame rate
fsz = 16; % Font size
errorSwitch = true; % Show standard deviation
pbSwitch = true; % Show progress bar during video generation
labyyLim = [0.95 1.2]; % Plot axis and video colour limits (stretch)
labxxLim = [0.95 1.2]; % Plot axis and video colour limits (stretch)
epsxxLim = [-0.2 0.2]; % Plot axis and video colour limits (strain)
epsyyLim = [-0.2 0.2]; % Plot axis and video colour limits (strain)

%% Create figure directory if it does not exist (yet)

if ~isdir(fDir)
    mkdir(fDir);
end

%% Colour map

cMapGreen = [215 48 39;...
             244 109 67;...
             253 174 97;...
             254 224 139;...
             255 255 191;...
             217 239 139;...]
```

```

166 217 106;...
102 189 99;...
26 152 80]/255;

cMapGreen = interp1((0:length(cMapGreen)-1)/(length(cMapGreen)-1), flip(cMapGreen), linspace(0,1,255));

%% Data properties

% Number of images
Ni = length(D.files);

% Number of points in x and y direction, respectively
Nxy = flip(size(D.cor(1).U1));
Nx = Nxy(1);    Ny = Nxy(2);

%% Coordinates in reference configuration

% Coordinates in column notation
X = D.cor(1).xroi';
Y = D.cor(1).yroi';

%% Displacement

% 2D Displacement fields
Ux = zeros(Ni, Nx, Ny);
Uy = zeros(Ni, Nx, Ny);

for inc = 2:Ni
    Ux(inc, :, :) = D.cor(inc-1).U1';
    Uy(inc, :, :) = D.cor(inc-1).U2';
end

%% Strain and stress calculations

% Preset
labXX = ones(Ni, Nx, Ny);    labYY = ones(Ni, Nx, Ny);
labYX = ones(Ni, Nx, Ny);    labXY = ones(Ni, Nx, Ny);
epsXX = zeros(Ni, Nx, Ny);    epsYY = zeros(Ni, Nx, Ny);
epsYX = zeros(Ni, Nx, Ny);    epsXY = zeros(Ni, Nx, Ny);

for inc = 2:Ni

    Exx = D.res(inc-1).Exx(:, :)';
    Eyy = D.res(inc-1).Eyy(:, :)';
    Eyx = D.res(inc-1).Eyx(:, :)';
    Exy = D.res(inc-1).Exy(:, :)';

    % Green-Lagrange strain
    epsXX(inc, :, :) = Exx;
    epsYY(inc, :, :) = Eyy;
    epsYX(inc, :, :) = Eyx;
    epsXY(inc, :, :) = Exy;

```

```

for iX = 1:size(X)
    for iY = 1:size(Y)
        % Green-Lagrange strain tensor
        E = [Exx(iX,iY) Eyx(iX,iY); Exy(iX,iY) Eyy(iX,iY)];

        % Right Cauchy-Green tensor
        C = 2*E + eye(2);

        % Stretches in xx and yy
        labXX(inc,iX,iY) = sqrt(C(1,1));
        labYY(inc,iX,iY) = sqrt(C(2,2));
    end
end
end

%% Plot displacement and stretch fields

if vidSwitch

    vidTotal = 3;

    [x, y] = meshgrid(X,Y);

    % Labxx
    cVar = labXX;
    vidName = 'labXX';
    cLim = labxxLim;
    imgVideoExport(D, x, y, Ux, Uy, cVar, nArrows, vidName, frameRate,...
        border, cMapGreen, cLim, fsz, fDir, vidFigSwitch, pbSwitch, 1,
vidTotal);

    % Labyy
    cVar = labYY;
    vidName = 'labYY';
    cLim = labyyLim;
    imgVideoExport(D, x, y, Ux, Uy, cVar, nArrows, vidName, frameRate,...
        border, cMapGreen, cLim, fsz, fDir, vidFigSwitch, pbSwitch, 2,
vidTotal);

    %% Labxx
    cVar = epsYY;
    vidName = 'epsYY';
    cLim = epsyyLim;
    imgVideoExport(D, x, y, Ux, Uy, cVar, nArrows, vidName, frameRate,...
        border, cMapGreen, cLim, fsz, fDir, vidFigSwitch, pbSwitch, 2,
vidTotal);

end

%% Compute mean stretches and their sdvs
labXXAvg = mean(mean(labXX,2),3);
labXXStd = std(std(labXX,0,2),0,3);

labYYAvg = mean(mean(labYY,2),3);
labYYStd = std(std(labYY,0,2),0,3);

```



```

labYXAvg = mean(mean(labYX,2),3);
labYXStd = std(std(labYX,0,2),0,3);

labXYAvg = mean(mean(labXY,2),3);
labXYStd = std(std(labXY,0,2),0,3);

%% Compute mean strain and their sdvs

epsXXAvg = mean(mean(epsXX,2),3);
epsXXStd = std(std(epsXX,0,2),0,3);

epsYYAvg = mean(mean(epsYY,2),3);
epsYYStd = std(std(epsYY,0,2),0,3);

%% Plot average stretches

h = figure('Visible','Off'); hold on; fsz = 20;

plot(0:Ni-1, labXXAvg, '-k')
plot(0:Ni-1, labYYAvg, '--k')
% plot(0:Ni-1, 1./sqrt(labYYAvg), ':k')
if errorSwitch
    errorbar(0:Ni-1,labXXAvg, labXXStd,'ok','MarkerEdgeColor',[0 0 0],
'MarkerFaceColor',[0 0 0],'MarkerSize',5)
    errorbar(0:Ni-1,labYYAvg, labYYStd,'sk','MarkerEdgeColor',[0 0 0],
'MarkerFaceColor',[1 1 1],'MarkerSize',5)
end

xlabel('Time point (-)','FontSize',fsz);
ylabel('Stretch (-)','FontSize',fsz);
set(gca,'FontSize',fsz);
l =
legend('\lambda_{xx}','\lambda_{yy}','Location','North','Orientation','horizontal');
set(l,'FontSize',fsz-4);
ylim(labxxLim)
xlim([0 Ni])
set(gca,'YTick',0.5:0.05:1.5)
print('-deps', h, strcat(fDir, 'gdic_plot_labxxyy'));

%% Plot average strains

h = figure('Visible','Off'); hold on; fsz = 20;

plot(0:Ni-1, epsXXAvg, '-k')
plot(0:Ni-1, epsYYAvg, '--k')
% plot(0:Ni-1, 1./sqrt(labYYAvg), ':k')
if errorSwitch
    errorbar(0:Ni-1,epsXXAvg, epsXXStd,'ok','MarkerEdgeColor',[0 0 0],
'MarkerFaceColor',[0 0 0],'MarkerSize',5)
    errorbar(0:Ni-1,epsYYAvg, epsYYStd,'sk','MarkerEdgeColor',[0 0 0],
'MarkerFaceColor',[1 1 1],'MarkerSize',5)
end

xlabel('Time point (-)','FontSize',fsz);
ylabel('Stretch (-)','FontSize',fsz);

```

```

set(gca,'FontSize',fsz);
l =
legend('\epsilon_{xx}','\epsilon_{yy}','Location','North','Orientation','horizontal');
set(l,'FontSize',fsz-4);
ylim(epsxxLim)
xlim([0 Ni])
% set(gca,'YTick',0.5:0.05:1.5)
print('-deps', h, strcat(fDir, 'gdic_plot_epsxxyy'));

%% Plot all stretches

h = figure('Visible','Off'); hold on; fsz = 20;

for iX = 1:20:Nx
    for iY = 1:20:Ny
        plot(0:Ni-1, labXX(:,iX,iY))
        plot(0:Ni-1, labYY(:,iX,iY))
    end
end

xlabel('Time point (-)','FontSize',fsz);
ylabel('Stretch (-)','FontSize',fsz);
set(gca,'FontSize',fsz);
ylim(labxxLim)
xlim([0 Ni])
set(gca,'YTick',0.5:0.05:1.5)
print('-depsc', h, strcat(fDir, 'gdic_plot_alllabs'));

%% Save workspace

D.gui = [];

close all
save(strcat(fDir, wkspName), 'Ux',
'Uy', 'labXX', 'labYY', 'epsXX', 'epsYY', 'Ni', 'labXXAvg', ...
'D')

```

A.1.2. Slidervideotoimages- Selection of frames

```
function SlidervideotoImages %Unfunctioned this for more interaction,
doesn't work

clc
clear all
close all

%%User Input
    imstep=30; %images after selected images
    step=1;
    filename='' % Filename here

%% Load Video

    vid=VideoReader(filename); % read movie
    % Get the number of frames, comment if hasframes method used
    NumFrames = vid.NumberOfFrames

%% Mathieu conversion to frames, OMS added pre-defining of matrix and
reading of only 1 color channel for speed & to conserve memory.

    MyMatrix=zeros(1080,1920,NumFrames,'uint8');
    for i = 1:1:NumFrames %convert movie to image frames, from 1:, by :1:
and up to :numframes
    %         i %counter
        % Read each frame
        frame = read(vid,i);
        % Add to 4D array
        MyMatrix(:,:,i)=frame(:,:,2); %(x, y, g, frame)
    end

%% OMS conversion to frames
%
%     MyMatrix=zeros(1080,1920,NumFrames,'uint8');
%     ii=1;
%     while hasFrame(vid)
%         frame = readFrame(vid);
%         MyMatrix(:,:,ii) = frame(:,:,2);
%         ii=ii+1
%     end
%

%% Initialize GUI

    % Get screensize
    screensize = get( groot, 'Screensize' );

    hFig = figure('Position',[100 100 screensize(3)-200 screensize(4)-
200],'Units','normalized');

    handles.axes1 = axes('Units','normalized','Position',[.2 .2 .6 .6]);
```

```

    %// Create GUI
    handles.SliderFrame = uicontrol('Style','slider','Position',[60 20
screensize(3)-300
50], 'Min',1, 'Max',NumFrames, 'Value',1, 'SliderStep',[1/NumFrames
2/NumFrames], 'Callback',@XSliderCallback);
    handles.SliderxListener =
addlistener(handles.SliderFrame, 'Value', 'PostSet', @(s,e)
XListenerCallback);

    % Get Frame
    handles.Text1 = uicontrol('Style','Text','Position',[60 75 60
30], 'String', 'Current frame');
    handles.Edit1 = uicontrol('Style','Edit','Position',[130 75 100
30], 'String', '1');
    handles.Ok1 =
uicontrol('Style','pushbutton','Position',[250,75,150,30], 'String', 'Choose
Frame', 'Callback', @done);

    %// Use setappdata to store the image stack

    setappdata(hFig, 'MyMatrix', MyMatrix);

    %// Display 1st frame
    imshow(MyMatrix(:, :, 1))

    %// Update handles structure.
    guidata(hFig, handles);

    %// Listener callback, executed when you drag the slider.

%% Callback function from GUI
function XListenerCallback

    %// Retrieve handles structure.
    handles = guidata(gcf);

    %// Get images
    MyMatrix = getappdata(hFig, 'MyMatrix');

    %// Get current frame
    CurrentFrame =
round((get(handles.SliderFrame, 'Value')));
    set(handles.Edit1, 'String', num2str(CurrentFrame));

    %// Display chosen frame.

    imshow(MyMatrix(:, :, CurrentFrame), 'Parent', handles.axes1);

    guidata(hFig, handles);
end

    %// Slider callback; executed when the slider is release or you
press
    %// the arrows.

```

```

function XSliderCallback(~,~)

    handles = guidata(gcf);

    %// Here retrieve MyMatrix using getappdata.
    MyMatrix = getappdata(hFig, 'MyMatrix');

    CurrentFrame =
round((get(handles.SliderFrame, 'Value')));
    set(handles.Edit1, 'String', num2str(CurrentFrame));

imshow(MyMatrix(:,:,CurrentFrame), 'Parent', handles.axes1);

    guidata(hFig, handles);
end

% Push button callback: frame selection
function done(~,~)
    handles = guidata(gcf);
    MyMatrix = getappdata(hFig, 'MyMatrix');
    % Get current frame
    CurrentFrame = round((get(handles.SliderFrame, 'Value')))

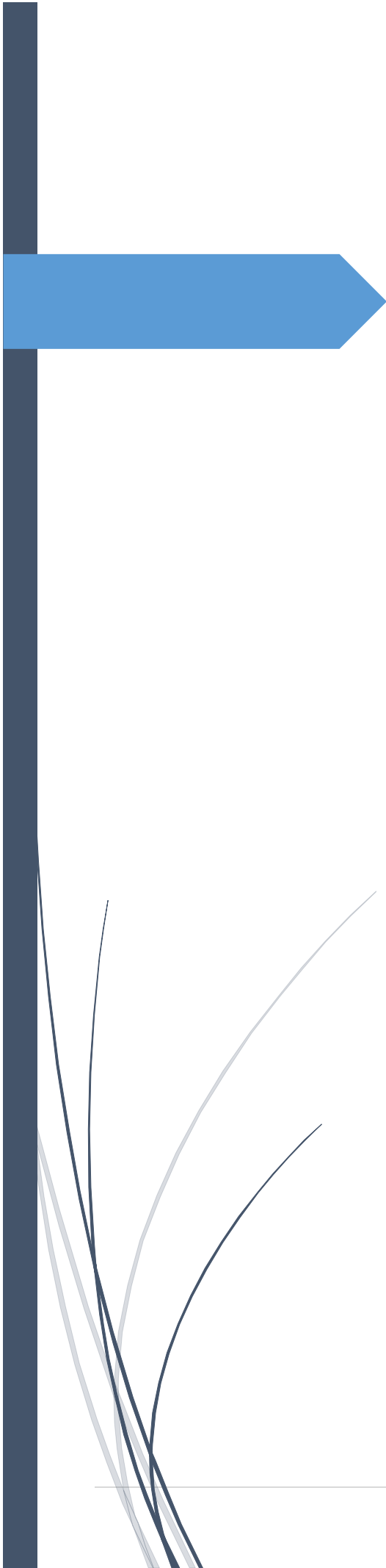
    % Make directory to store images and go into this directory
    mkdir([filename, '_selected images/'], int2str(CurrentFrame))
    cd([filename, '_selected images/', int2str(CurrentFrame)])

    % Store images
    for im=CurrentFrame:step:CurrentFrame+imstep
        % Get image
        image=MyMatrix(:,:,im); %3rd dimension was RGB, now all
is green
        % Save image
        imwrite(image, [filename, num2str(im-
CurrentFrame+1), '.jpg'])
    end
    % close the GUI
    %close all
    % back to base folder
    cd ../../
end

end

```

A.1.3. LITERARY REVIEW



Macrophage-induced HVSC migration in 3D scaffolds with variable fiber alignment and cyclic stretch

Sparla, J.K.W.
TUE

Table of Contents

Introduction	38
Hypothesis.....	41
Methods.....	42
Overview	42
Creating the scaffolds	42
Measuring the migration	43
Determining the effect of cyclic stretch on migration.....	43
Cytokine release profiles.....	44
Experiments timeline	44
Reference list:	45

9 Introduction

In the Netherlands approximately 1% of the population suffers from renal failure, with 2000 new patients every year [1]. Chronic kidney disease (CKD) is a progressive loss in kidney function and if left untreated, results in death. CKD can be classified by severity in five stages. The fifth stage of this disease is called end stage renal disease (ESRD). Patients suffering from ESRD have a renal functionality below 10% of normal capacity and rely on renal replacement therapies or haemodialysis[2]. Worldwide, two million people are being treated for ESRD, requiring haemodialysis or a kidney transplant to stay alive[3]. Haemodialysis is necessary at low renal functionality (<15% functionality) due to the kidneys not removing enough wastes and fluid from your blood anymore [4]. During the process of haemodialysis, blood directly from your circulation is run through a dialysis machine which contains a filter[4]. The blood flow access is created via a minor surgery in the forearm of a patient. So, in order to perform haemodialysis adequate access to blood flow is required. Currently, the golden standard to create haemodialysis access is connecting an artery to a vein creating an arteriovenous fistula (AVF). A disadvantage of the AVF is its inability to be used acutely, since AVFs require a maturation phase of three to four months to adjust to the augmented blood flow and to induce vessel wall thickening[5]. On top of this disadvantage, 60% of the AVFs also fail to mature adequately.

A different way to gain access to the blood flow is to make use of synthetic arteriovenous-grafts (AVG). In this way, a tubular construct is used to connect an artery to a vein as opposed to directly connecting them. This creates an artificial fistula and increases blood flow for haemodialysis cannulation[6].

However, the implantation of AV-grafts is also not without disadvantages. Currently, AVGs have a high incidence of thrombosis, infection and the occurrence of neointimal hyperplasia, which leads to venous stenosis[7].

Novel approaches to gain vascular access involve the use of tissue engineering (TE). Tissue engineered constructs can be tailored to requirements which can aid in preventing the complications encountered by synthetic AVGs. Wystrychowski et al. [8] created the first clinical use of a tissue engineered construct for vascular access by using TE vascular grafts built from allogenic fibroblasts. Clinical use of this graft showed overall good results and no access-related infections. A drawback to this approach however, is the long production time(7,5 months), so failure to use acutely. This problem could be prevented by using an in-situ TE approach.

In-situ TE uses resorbable biomaterials with attached cues to recruit cells in vivo, to induce endogenous tissue formation and maintain tissue homeostasis [9]. So, by using in-situ to create AVGs, these biomaterials with attached cues (scaffolds) can be created on demand in large quantities beforehand. In this way, in-situ TE AVGs can be used acutely.

The implantation of any foreign material into living tissue however, like the implantation of an in-situ tissue engineered AVG, is bound to evoke a host inflammatory response also known as the foreign body response (FBR)[10]. This FBR is a series of cell-based signaling events. Macrophages are one of the key players in the FBR. These macrophages function as mediators of the formation and remodeling of tissue by secreting various essential growth factors and/or cytokines which can promote or inhibit tissue formation. These key growth factors and cytokines for example include TGF- β , TNF- α , matrix metalloproteases (MMPs) and PDGF. Which factors are secreted by the macrophages at what point in time, depends on the physical properties of the environment (e.g. stiffness) and the chemical environment of the macrophages(e.g. cytokines), which in turn determines the phenotype of the macrophage.

There are two distinct phenotypes generally described in literature. These include a pro inflammatory phenotype “M1 macrophage” and a pro-wound healing phenotype “M2 macrophage”.

The M2 phenotype can then again be sub-divided into three different phenotypes (M2a, M2b and M2c). However, all of these different phenotypes tend to overlap, making it difficult to identify individual macrophage phenotype[11]. The balance between M2/M1 macrophages present in implanted biomaterials during the FBR, is a predictor for long term tissue outcome[9], making modulation of macrophage phenotype a key target to guide functional tissue regeneration. It has been well established that macrophages physically and chemically (via exchange of cytokines) interact with other cell types, like VMSCs and (myo-)fibroblasts[12,13]. Some of these interactions are depicted in figure 1 .

These interactions are important for the foreign body response, which causes these interactions to be the focus for many researchers. Multiple studies using in vitro co-cultures have unraveled paracrine signaling mechanisms and routes between macrophages, fibroblasts and SMCs in 2D as well as 3D scaffold environments[9]. Knowledge regarding these signaling mechanisms is a must in order to create functional TE constructs, like in-situ TE AVGs.

There are many factors which can influence the phenotype of cells like macrophages and as a consequence of this, can influence the cytokine or growth factor secretion of cells like VMSCs and (myo)fibroblasts due to their interactions with each other.

Since cells under physiological conditions are constantly subjected to forces in vivo, it was discovered that applying cyclic stretch to macrophages, has an effect on the phenotype of these macrophages. This change in phenotype is caused by the change induced in cellular morphology as a result of the mechanical stress on the macrophage. It has been shown that a uniaxial cyclic stretch of 10% causes alignment and elongation of the macrophages in the direction of the applied cyclic stretch [14]. In different research by Ballotta et al. [15] applying cyclic stretch to macrophages in physiological ranges(5-12%)[16], has also been shown to directly affect macrophage phenotype. For example, a strain of 7% was shown to guide macrophage polarization to the M2 phenotype, whilst at strains of 12% less M2 macrophages are present[15]. This change in macrophage phenotype as a consequence of the cyclic stretch in turn changes the cytokine release profile of the macrophages and in turn the interactions of macrophages with other cell types.

Another important set of parameters which can alter the polarization of macrophages, are fiber size, fiber alignment and pore size of the scaffold used for tissue engineering[9].

It has for example been shown that a positive correlation exists between the pore size of a scaffold seeded with macrophages and the polarization of these macrophage towards an M2 phenotype, with 20–40 μm being the most favorable pore size to promote M2 polarization[17]. Aside from this, it was shown that an increasing pore size caused increased expression of angiogenic factors (VEGF, bFGF, TGF- β)[18].

Scaffold fiber size also influences phenotype of macrophages when seeded on these scaffolds. Fibers larger than 5 μm have been shown to polarize towards M2 phenotype, whereas scaffolds with smaller fibers have been shown to have a more M1 phenotype [19].

It should be noted however, that scaffold fiber size and scaffold pore size are dependent on each other, since larger fibers also increase the scaffold pore size. This often causes contradictions of expected macrophage phenotype in literature.

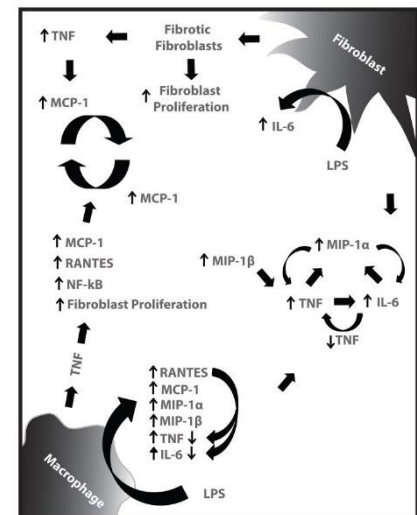


Figure 2, different signaling interactions between macrophages and fibroblasts

Macrophage phenotype has also been shown to be affected by using topographical cues in 2D using microgrooves with dimensions of 400-500 nm in width and 0.8 μm -1.3 μm in height [20]. This effect is caused by the cells ability to align in the direction of microgrooves. This alignment onto the microgrooves causes the macrophages to elongate, which in turn causes them to assume a more M2-like phenotype.

For this reason, fiber alignment in 3D possibly also affects macrophage polarization this however has not yet been proven since precise fiber alignment in 3D is hard to control.

Since all of these factors mentioned above modulate macrophage phenotype and cytokine secretion, they are important considerations when trying to modulate the foreign body response as well as when designing in-situ TE AVGs. This knowledge can be used to solve some of the problems that occur in synthetic non-TE AVGs.

One of the problems with these synthetic AVGs was the occurrence of neointimal hyperplasia, which is caused by the migration of SMCs and FBs from the media into the intima layer[21]. What the exact underlying cause is for the migration of these two cell types is not yet known. However, vascular injury (e.g. as a result of implantation) as well as altered fluid flow and shear stress seem to play a role in causing neointimal hyperplasia by activating FBs and SMCs, causing them to migrate[21]. What is known is that macrophages interact in paracrine (via e.g. cytokines) and juxtacrine (via direct contact) ways with SMCs and FBs and that they affect the migration of these two cell types[12,13]. For this reason, it is important to know what effect the factors mentioned above (fiber alignment, cyclic stretch, pore and fiber size) indirectly (via macrophages) have on the FBs or SMCs.

This also brings forth the research question addressed in this review:

“What is the contribution of fiber alignment and cyclic stretch on macrophage-induced HVSC migration in a 3D environment?”

In this research, instead of using SMCs and FBs, human adult vena saphena (HVSCs) will be used. These HVSCs are cells derived from the saphenous vein and are comparable to myofibroblasts. On top of this, in the study performed by Schnell et al. [22], these cells showed superior collagen formation compared to aortic derived myofibroblasts. Tissue derived constructs created by the HVSCs also had better mechanical properties than the aortic derived myofibroblasts. These two properties (increased collagen production and enhanced mechanical properties in TE constructs) are useful for in-situ TE AVGs, since these AVGs require collagen production in the remodeling process of the scaffold in vivo. They also are required to be resilient enough to function as blood vessels, which requires good mechanical properties. Since these cells are a more available source compared to the aortic derived cells, they are a promising alternative for cardiovascular tissue engineering.

To answer this research question, I divide it into several smaller research questions to separately address alignment and cyclic stretch.

“To what extent does fiber alignment contribute to macrophage-induced HVSC migration?”

“To what extent does cyclic stretch contribute to macrophage-induced HVSC migration?”

“What is the effect of combining both cyclic stretch and fiber alignment on macrophage-induced HVSC migration?”

The knowledge regarding the effects that fiber alignment and cyclic stretch and the combination of both have on macrophage-induced HVSC migration, can be taken into account when designing an in-situ TE AVG.

10 Hypothesis

In previous studies, in which macrophages were co-cultured with VSMCs, the overall outcome was that VSMC migration and infiltration into a degradable polyurethane (D-PHI) scaffold was increased by macrophages which had a more M2 secretory profile [23].

For this reason, it is hypothesized that the polarization of macrophages to an M2 state, causes an increase in migration compared to the M0 or M1 polarization state and compared to migration of a mono-culture of HVSCs.

VSMCs are comparable to HVSCs, due to both cells having migratory and contractile phenotypes and both expressing α -sma in their contractile phenotypes.

Due to the fact that aligned microgrooves in 2D with dimensions of 400 to 500 nm in width and 0.8 μ m to 1.3 μ m in height [20] can cause M2 macrophage polarization (as mentioned before in the introduction), it is assumed that macrophages when cultured in 3D fiber anisotropically aligned scaffolds also polarize towards a more M2 like phenotype. Further experiments will need to confirm this assumption. For this reason, a scaffold with isotropically (randomly) aligned fibers is thought to have more M1 like macrophages.

Building on the assumptions mentioned above, it can be hypothesized that anisotropic fiber alignment increases macrophage-induced HVSC migration compared to isotropic fiber alignment and compared to migration of a mono-culture of HVSCs.

Low strains of values <7% have been shown to guide macrophages towards a more reparative M2 phenotype, whilst high strain values (12%) caused a decrease in M2 macrophage amount (described in introduction).

Due to this information and assuming M2 macrophages increase HVSC migration, it is hypothesized that low cyclic stretch values (<7%) cause an increase in HVSC migration, whilst high values of cyclic stretch (12%) cause a decrease in HVSC migration.

The combination of both alignment and cyclic stretch is hypothesized to cause different amounts of macrophage induced-HVSC migration compared to each of these factors individually.

Mechanical cues that polarize macrophages to an M2 state, for example anisotropic fiber alignment within the scaffold, can conflict with cues that polarize macrophages to an M1 state, for example high values of cyclic strain(12%). Mechanical cues can also overlap if both of the cues given to the macrophages polarize macrophages to an M2 state.

It is therefore hypothesized that conflicting mechanical cues decrease the macrophage-induced HVSC migration and that overlapping mechanical cues increase the macrophage-induced HVSC migration compared to individual mechanical cues.

Methods

10.1 Overview

Initially, both required cell types (HVSCs and monocytes) will be isolated and cultured separately. PCL-bisurea (PCLbu) scaffolds (with anisotropic and isotropic fibers) will be then created by using electrospinning. After the scaffolds are created and cells have been cultured, the macrophage-induced HVSC migration will be quantified by using the main experimental setup depicted in figure 3. In this setup, the cultured HVSCs will be seeded onto a Transwell porous membrane, below this membrane, the cultured macrophages will be seeded onto the electrospun scaffold. This scaffold will then be exposed to cyclic stretch, during this stretching, HVSCs will be allowed to migrate for periods of time, after which the HVSCs that migrated through the pores, will be stained and counted. | All experiments will be performed in triplo unless specified otherwise in the description.

Cell isolation experiments

Monocytes will be isolated from buffy coats. To achieve this isolation, PBMCs firstly have to be isolated from the buffy coats by using Lymphoprep (hydrophilic polysaccharides that separate layers of blood) combined with gradient centrifugation to separate the different cells. The PBMCs will be extracted and further isolated by using pan-macrophage MACs, in which all cells but macrophages will be tagged by magnetic microbeads. This solution will then be run through a MACs column placed in a MACs separator(magnetic plate). A good indication of successful isolation can be obtained by comparing the percentage of obtained cells with the physiological values (10-20%).

Culturing the cells

The macrophages with different phenotypes will be created by culturing monocytes in well plates for 7 days with an initial seeding density of $1,5 \times 10^5$ cells/cm² per well. The macrophages will then be allowed to polarize for 18 hours towards M1 or M2 polarization by adding IFN γ (M1) or IL-4(M2). A control will also be made in which monocytes will be cultured without adding any cytokines (M0). The phenotype of these polarized macrophages will be confirmed by using qPCR. The HVSCs will be cultured as described by Turner et al[24].

Creating the scaffolds

Scaffolds will be made from the material PCL-bisurea (PCLbu), which consists of polycaprolactone (PCL) and bisurea groups (bu). This material is a biomaterial aimed for use in cardiovascular tissue engineering PCL[25]. PCLbu is also fatigue resistant for more than 3 million cycles at 10% elongation, which is a useful characteristic for cardiovascular applications[26].

The scaffolds will be made by using electrospinning with fibers of around 3-5 μ m in size, this fiber size was chosen to minimize macrophage M1 and M2 polarization (see introduction).

Since the exact fiber size created during electrospinning is hard to control, the actual size will be determined by using Scanning Electron Microscopy (SEM).

Using this technique, two differently fiber aligned scaffolds will be made. In one scaffold, fibers will be aligned isotopically whilst in the other scaffold the fibers will be aligned anisotropically.

10.2 Measuring the migration

The migration of the HVSCs will be determined by using Boyden chamber assays using Transwell permeable membranes[27]. Transwell membranes made of Polyester (PET) with a pore size of 8 μm will be used since cells on PET membranes are more clearly visible. The pore size of 8 μm was chosen since this is the biggest available pore size and HVSCs are large cells[27]. This experiment will be performed in several different scenarios.

In the first experimental setup (depicted in Figure 2), HVSCs will be cultured on the Transwell membrane above wells filled with macrophage derived medium (MDM). This medium will be extracted from macrophages of different phenotypes(M0, non-stimulated/M1/M2).

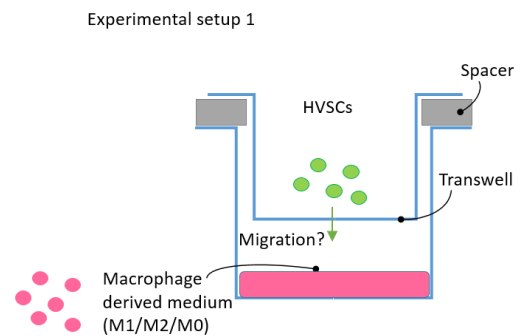


Figure 3, Experimental setup 1 (property of Anthal Smits)

The migration of these HVSCs will then be measured by using a Boyden chamber assay. In which they are allowed to migrate for 18 hours, 24 hours and 2 days after which the amount of migrated cells will be measured. This cell amount will be determined by staining the migrated cells with a cytological dye and then counting the amount of stained cells.

These specific time points were chosen based on experiments done with similar cell types (Smooth muscle cells)[23]. Three different time points were chosen here, due to optimal time to determine macrophage-induced HVSC migration not yet having been determined.

A control setup with HVSCs in mono-culture, without any stimulatory particles in the wells below will also be performed to experimental results.

In the second scenario (depicted in figure 3), instead of using MDM, M0 macrophages will be used and seeded onto the different electrospun scaffolds (isotropic, anisotropic). The scaffold will be located in different wells plates below the Transwell membrane seeded with HVSCs. Similarly as in the first experimental setup, a Boyden chamber assay will be performed using the same time points (18 hours, 24 hours and 2 days).

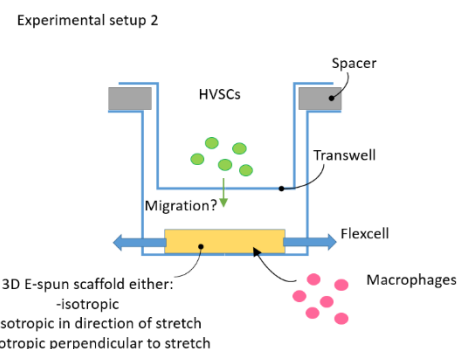


Figure 4, Experimental setup 2 (property of Anthal Smits)

After this period the scaffold will be rinsed with trypsin to detach the cells from scaffold.

Cells will be stained with a cytological dye and the amount of stained cells will be counted.

Determining the effect of cyclic stretch on migration

To determine the effect of stretch on macrophage-induced HVSC migration, the same experimental setup depicted in figure 3 will be used, this time however cyclic stretch will be applied on the different electrospun scaffolds (isotropic, anisotropic in direction of stretch and anisotropic perpendicular to stretch). A range of cyclic stretches with values of 4%, 7% and 12% will be applied on all three mentioned electrospun scaffolds. This cyclic stretch will be applied using the Flexcell FX-5000 Tension system at the same time points mentioned in the second experiment (18 hours, 24 hours and 2 days). The amount of migrated HVSCs will once again be quantified using the methods described above in the second experiment.

Cytokine release profiles

The amount of cytokines released during the three different experiments will be measured at different time points ($t=0$, $t=18$ hours, $t=24$ hours, $t=2$ days). By using the same time points in all three experiments and in the cytokine assay, correlations between upregulated cytokines and the amount of macrophage-induced HVSC migration can be found.

This amount of released cytokines will be measured by using a multiplex ELISA assay, which allows the measuring of multiple cytokines at the same time.

The concentrations of the following cytokines will be measured : RANTES, TNF, MCP-1, MIP1- β , MIP1- α , IL-6, IL-2, IL-4, IL-5, IL-9, IL-10, IL-12P70, IL-13, and IFN- γ . These cytokines will be tested due to their involvement in the interactions between fibroblasts and macrophages as well as in the migration of fibroblasts[28].

10.3 Experiments timeline

To provide more structure of which experiments are done when and to keep the experiments on schedule, a timeline of the experiments has been made (depicted in figure 4).

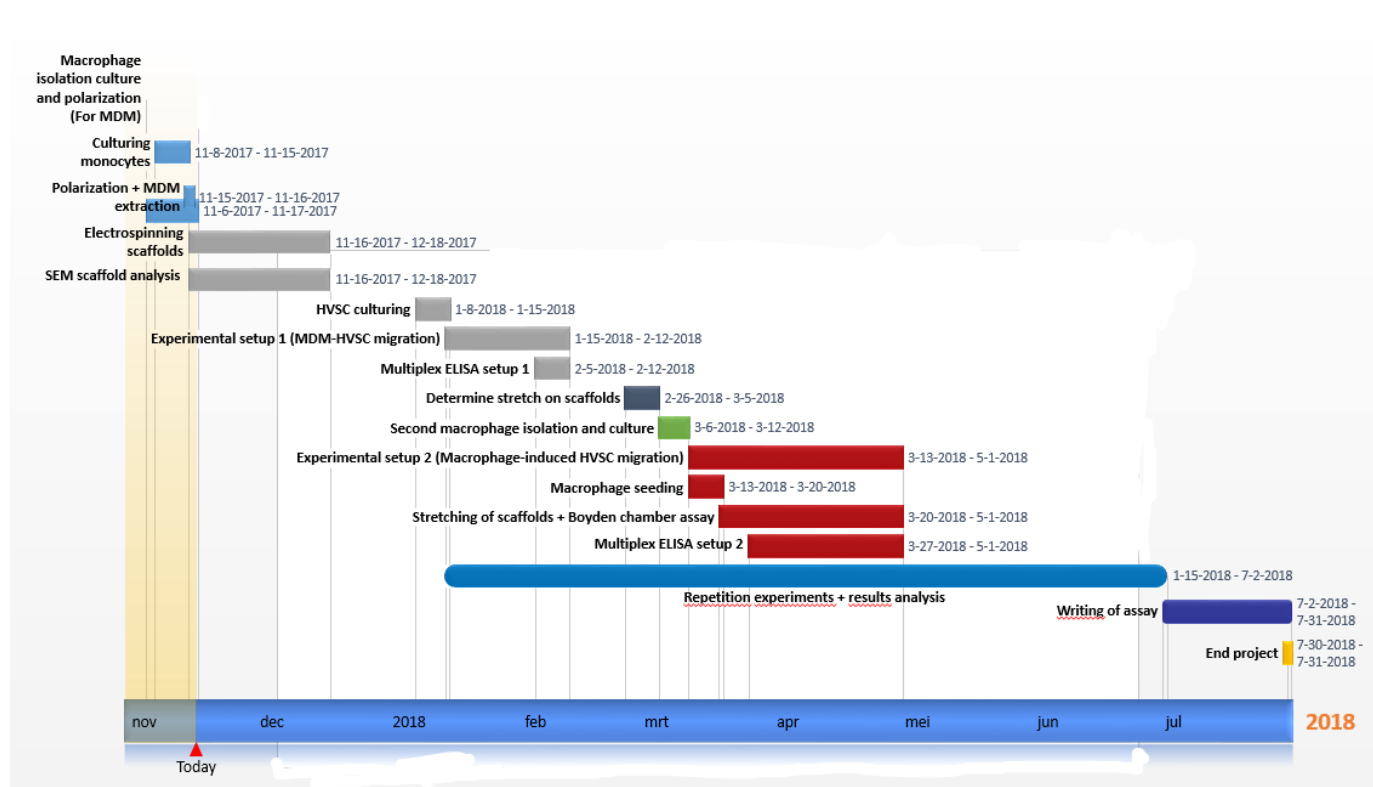


Figure 5, Timeline depicting all planned experiments

Reference list:

- [1]:Anon, (2017). [online] Available at: <https://www.nierstichting.nl/leven-met-een-nierziekte/feiten-en-cijfers/> [Accessed 14 Nov. 2017].
- [2]:The National Kidney Foundation. (2017). End Stage Renal Disease in the United States. [online] Available at: <https://www.kidney.org/news/newsroom/factsheets/End-Stage-Renal-Disease-in-the-US> [Accessed 3 Nov. 2017].
- [3]: The National Kidney Foundation. (2017). Global Facts: About Kidney Disease. [online] Available at: <https://www.kidney.org/kidneydisease/global-facts-about-kidney-disease> [Accessed 14 Nov. 2017].
- [4]: The National Kidney Foundation. (2017). Hemodialysis. [online] Available at: <https://www.kidney.org/atoz/content/hemodialysis> [Accessed 17 Nov. 2017]
- [5]: Rosas, S. E., & Feldman, H. I. (2012). Synthetic vascular hemodialysis access vs native arteriovenous fistula: A cost-utility analysis. *Annals of Surgery*, 255(1), 181–186. <http://doi.org/10.1097/SLA.0b013e31822f4e9b>
- [6]: Anon, (2017). Vascular Access for Hemodialysis. [online] Available at: <https://www.niddk.nih.gov/health-information/kidney-disease/kidney-failure/hemodialysis/vascular-access> [Accessed 3 Nov. 2017].
- [7]: Peck, M. K., Dusserre, N., Zagalski, K., Garrido, S. A., Wystrychowski, W., Glickman, M. H., ... & McAllister, T. N. (2010). New biological solutions for hemodialysis access. *The journal of vascular access*, 12(3), 185-192.
- [8]: Wystrychowski, W., McAllister, T. N., Zagalski, K., Dusserre, N., Cierpka, L., & L'heureux, N. (2014). First human use of an allogeneic tissue-engineered vascular graft for hemodialysis access. *Journal of vascular surgery*, 60(5), 1353-1357.
- [9]: Wissing, T., Bonito, V., Bouten, C. and Smits, A. (2017). Biomaterial-driven in situ cardiovascular tissue engineering—a multi-disciplinary perspective. *npj Regenerative Medicine*, 2(1).
- [10]: Anderson, J. M., Rodriguez, A., & Chang, D. T. (2008). FOREIGN BODY REACTION TO BIOMATERIALS. *Seminars in Immunology*, 20(2), 86–100. <http://doi.org/10.1016/j.smim.2007.11.004>
- [11]: Mosser, D. M., & Edwards, J. P. (2008). Exploring the full spectrum of macrophage activation. *Nature reviews immunology*, 8(12), 958-969.
- [12]: Sophie Van Linthout, Kapka Miteva, Carsten Tschöpe; Crosstalk between fibroblasts and inflammatory cells, *Cardiovascular Research*, Volume 102, Issue 2, 1 May 2014, Pages 258–269, <https://doi.org/10.1093/cvr/cvu062>
- [13]: K.G. Battiston, R.S. Labow, C.A. Simmons, J.P. Santerre (2015), Immunomodulatory polymeric scaffold enhances extracellular matrix production in cell co-cultures under dynamic mechanical stimulation, In *Acta Biomaterialia*, Volume 24, 2015, Pages 74-86, ISSN 1742-7061, <https://doi.org/10.1016/j.actbio.2015.05.038>.
- [14]: Oya, K., Sakamoto, N., & Sato, M. (2013). Hypoxia suppresses stretch-induced elongation and orientation of macrophages. *Bio-medical materials and engineering*, 23(6), 463-471.
- [15]: Ballotta, V., Driessen-Mol, A., Bouten, C. V. C. & Baaijens, F. P. T. Strain-dependent modulation of macrophage polarization within scaffolds. *Biomaterials*. 35, 4919–4928 (2014).
- [16]: Liu, X. M., Peyton, K. J., & Durante, W. (2013). Physiological cyclic strain promotes endothelial cell survival via the induction of heme oxygenase-1. *American Journal of Physiology-Heart and Circulatory Physiology*, 304(12), H1634-H1643.
- [17]: Madden, L. R. et al. Proangiogenic scaffolds as functional templates for cardiac tissue engineering. *Proc. Natl. Acad. Sci. U. S. A.* 107, 15211–15216 (2010).
- [18]: Garg, K., Pullen, Na, Oskeritzian, Ca, Ryan, J. J. & Bowlin, G. L. Macrophage functional polarization (M1/M2) in response to varying fiber and pore dimensions of electrospun scaffolds.

Biomaterials. 34, 4439–4451 (2013).

[19]: Wang, Z., Cui, Y., Wang, J., Yang, X., Wu, Y., Wang, K., Gao, X., Li, D., Li, Y., Zheng, X., Zhu, Y., Kong, D. and Zhao, Q. (2014). The effect of thick fibers and large pores of electrospun poly(ϵ -caprolactone) vascular grafts on macrophage polarization and arterial regeneration. *Biomaterials*, 35(22), pp.5700-5710.

[20]: Luu, T. U., Gott, S. C., Woo, B. W. K., Rao, M. P., & Liu, W. F. (2015). Micro and Nano-patterned Topographical Cues for Regulating Macrophage Cell Shape and Phenotype. *ACS Applied Materials & Interfaces*, 7(51), 28665–28672. <http://doi.org/10.1021/acsami.5b10589>

[21]: Shi, Z.-D., & Tarbell, J. M. (2011). Fluid Flow Mechanotransduction in Vascular Smooth Muscle Cells and Fibroblasts. *Annals of Biomedical Engineering*, 39(6), 1608–1619. <http://doi.org/10.1007/s10439-011-0309-2>

[22]: Schnell, A., Hoerstrup, S., Zund, G., Kolb, S., Sodian, R., Visjager, J., Grunenfelder, J., Suter, A. and Turina, M. (2001). Optimal Cell Source for Cardiovascular Tissue Engineering: Venous vs. Aortic Human Myofibroblasts. *The Thoracic and Cardiovascular Surgeon*, 49(04), pp.221-225.

[23]: Battiston, K., Ouyang, B., Labow, R., Simmons, C. and Santerre, J. (2014). Monocyte/macrophage cytokine activity regulates vascular smooth muscle cell function within a degradable polyurethane scaffold. *Acta Biomaterialia*, 10(3), pp.1146-1155.

[24]: Turner, N. A., Ho, S., Warburton, P., O'Regan, D. J., & Porter, K. E. (2007). Smooth muscle cells cultured from human saphenous vein exhibit increased proliferation, invasion, and mitogen-activated protein kinase activation in vitro compared with paired internal mammary artery cells. *Journal of vascular surgery*, 45(5), 1022-1028.

[25]: M.H. Van, M. (n.d.). Electrospinning of Scaffolds for Cardiovascular Tissue Engineering.[online] Available at: <http://mate.tue.nl/mate/pdfs/6330.pdf> [Accessed 3 Nov. 2017].

[26]: Electrospinning Partner | IME Technologies. (2017). Marc Simonet | Electrospinning Techniques For Regenerative Medicine. [online] Available at: <https://www.imetechnologies.com/marc-simonet-electrospinning-techniques/> [Accessed 3 Nov. 2017].

[27]: Csmedia2.corning.com. (2017). [online] Available at: http://csmedia2.corning.com/LifeSciences/Media/pdf/transwell_guide.pdf [Accessed 3 Nov. 2017].

[28]: Holt, D. J., Chamberlain, L. M., & Grainger, D. W. (2010). Cell-cell signaling in co-cultures of macrophages and fibroblasts. *Biomaterials*, 31(36), 9382–9394. <http://doi.org/10.1016/j.biomaterials.2010.07.101>